

1 **Mitochondrial respiratory states and rates:**
2 **Building blocks of mitochondrial physiology**

3 Part 1. MitoEAGLE preprint 2018-03-01(32)

4
5 http://www.mitoeagle.org/index.php/MitoEAGLE_preprint_2018-02-08

6 Preprint version 32 (2018-03-01)

7
8 **MitoEAGLE Network**

9 Corresponding author: Gnaiger E

10 Co-authors:

11 Aasander Frostner E, Acuna-Castroviejo D, Ahn B, Alves MG, Amati F, Aral C,
12 Arandarčikaitė O, Bailey DM, Bakker BM, Bastos Sant'Anna Silva AC, Battino M, Beard
13 DA, Ben-Shachar D, Bishop D, Borsheim E, Borutaitė V, Breton S, Brown GC, Brown RA,
14 Buettner GR, Burtscher J, Calabria E, Calbet JA, Calzia E, Cardoso LHD, Carvalho E,
15 Casado Pinna M, Cervinkova Z, Chang SC, Chaurasia B, Chen Q, Chicco AJ, Chinopoulos C,
16 Clementi E, Coen PM, Collin A, Crisóstomo L, Das AM, Davis MS, De Palma C, Dias TR,
17 Distefano G, Doerrier C, Drahota Z, Duchon MR, Durham WJ, Ehinger J, Elmer E, Endlicher
18 R, Fell DA, Ferko M, Ferreira JCB, Ferreira R, Filipovska A, Fisar Z, Fischer M, Fisher JJ,
19 Fornaro M, Galkin A, Garcia-Roves PM, Garcia-Souza LF, Garten A, Genova ML, Giovarelli
20 M, Gonzalez-Armenta JL, Gonzalo H, Goodpaster BH, Gorr TA, Gourlay CW, Granata C,
21 Grefte S, Haas CB, Haavik J, Han J, Harrison DK, Hellgren KT, Hernansanz-Agustin P,
22 Holland OJ, Hoppel CL, Houstek J, Hunger M, Iglesias-Gonzalez J, Irving BA, Iyer S,
23 Jackson CB, Jadiya P, Jang DH, Jansen-Dürr P, Jespersen NR, Jha RK, Kaambre T, Kane
24 DA, Kappler L, Karabatsiakakis A, Keijer J, Keppner G, Khamoui AV, Klingenspor M,
25 Komlodi T, Koopman WJH, Kopitar-Jerala N, Krajcova A, Krako Jakovljevic N, Kuang J,
26 Kucera O, Labieniec-Watala M, Lai N, Laner V, Larsen TS, Lee HK, Leeuwenburgh C,
27 Lemieux H, Lerfall J, Liu J, Lucchinetti E, MacMillan-Crow LA, Makrecka-Kuka M, Malik
28 A, Markova M, Meszaros AT, Michalak S, Moiso N, Molina AJA, Montaigne D, Moore AL,
29 Moreira BP, Mracek T, Muntane J, Muntean DM, Murray AJ, Nemeč M, Neuzil J, Newsom
30 S, Nozickova K, O'Gorman D, Oliveira MT, Oliveira PF, Oliveira PJ, Orynbayeva Z, Pak
31 YK, Palmeira CM, Patel HH, Pecina P, Pelnena D, Pereira da Silva Grilo da Silva F, Pesta D,
32 Petit PX, Pichaud N, Piel S, Pirkmajer S, Porter RK, Pranger F, Prochownik EV,
33 Pulinilkunnil T, Puurand M, Radenkovic F, Radi R, Ramzan R, Reboredo P, Renner-Sattler
34 K, Robinson MM, Rohlena J, Rolo AP, Ropelle ER, Røslund GV, Rossiter HB, Rybacka-
35 Mossakowska J, Saada A, Safaei Z, Salvadego D, Sandi C, Scatena R, Schartner M,
36 Scheibye-Knudsen M, Schilling JM, Schlattner U, Schönfeld P, Schwarzer C, Scott GR,
37 Shabalina IG, Sharma P, Sharma V, Shevchuk I, Siewiera K, Silber AM, Singer D, Smenes
38 BT, Soares FAA, Sobotka O, Sokolova I, Spinazzi M, Stankova P, Stier A, Stocker R,
39 Sumbalova Z, Suravajhala P, Swerdlow RH, Swiniuch D, Tanaka M, Tandler B, Tavernarakis
40 N, Tepp K, Thyfault JP, Tomar D, Towheed A, Tretter L, Trifunovic A, Trivigno C, Tronstad
41 KJ, Trougakos IP, Tyrrell DJ, Urban T, Valentine JM, Velika B, Vendelin M, Vercesi AE,
42 Victor VM, Villena JA, Vitorino RMP, Vogt S, Volani C, Votion DM, Vujacic-Mirski K,
43 Wagner BA, Ward ML, Watala C, Wei YH, Wieckowski MR, Williams C, Wohlwend M,
44 Wolff J, Wuest RCI, Zaugg K, Zaugg M, Zischka H, Zorzano A

45
46 Supporting:

47 Bernardi P, Boetker HE, Bouitbir J, Coker RH, Dubouchaud H, Dyrstad SE, Engin AB, Gan
48 Z, Garlid KD, Haendeler J, Hand SC, Hepple RT, Hickey AJ, Hoel F, Kainulainen H,
49 Kowaltowski AJ, Lane N, Lenaz G, Liu SS, Mazat JP, Menze MA, Methner A, Nedergaard J,
50 Pallotta ML, Parajuli N, Pettersen IK, Porter C, Salin K, Sazanov LA, Skolik R, Sonkar VK,
51 Szabo I, Vieyra A

Updates and discussion:

http://www.mitoeagle.org/index.php/MitoEAGLE_preprint_2018-02-08

Correspondence: Gnaiger E

Chair COST Action CA15203 MitoEAGLE – <http://www.mitoeagle.org>

*Department of Visceral, Transplant and Thoracic Surgery, D. Swarovski Research
Laboratory, Medical University of Innsbruck, Innrain 66/4, A-6020 Innsbruck, Austria*

Email: mitoeagle@i-med.ac.at

Tel: +43 512 566796, Fax: +43 512 566796 20

Contents**Abstract****Executive summary****1. Introduction** – Box 1: In brief: Mitochondria and Bioblasts**2. Oxidative phosphorylation and coupling states in mitochondrial preparations**

Mitochondrial preparations

2.1. Respiratory control and coupling

The steady-state

Specification of biochemical dose

Phosphorylation, P_{\gg} , and P_{\gg}/O_2 ratio

Control and regulation

Respiratory control and response

Respiratory coupling control and ET-pathway control

Coupling

Uncoupling

2.2. Coupling states and respiratory rates

Respiratory capacities in coupling control states

LEAK, OXPHOS, ET, ROX

Quantitative relations

2.3. Classical terminology for isolated mitochondria

States 1–5

3. Normalization: fluxes and flows*3.1. Normalization: system or sample*

Flow per system, I

Extensive quantities

Size-specific quantities – Box 2: Metabolic fluxes and flows: vectorial and scalar

3.2. Normalization for system-size: flux per chamber volume

System-specific flux, J_{V,O_2}

3.3. Normalization: per sample

Sample concentration, C_{mX}

Mass-specific flux, $J_{O_2/mX}$

Number concentration, C_{NX}

Flow per object, $I_{O_2/X}$

3.4. Normalization for mitochondrial content

Mitochondrial concentration, C_{mtE} , and mitochondrial markers

Mitochondria-specific flux, $J_{O_2/mtE}$

*3.5. Evaluation of mitochondrial markers**3.6. Conversion: units***4. Conclusions** – Box 3: Definitions: Mitochondrial and cell respiration**5. References**

103 **Abstract** As the knowledge base and importance of mitochondrial physiology to human health
104 expands, the necessity for harmonizing nomenclature concerning mitochondrial respiratory
105 states and rates has become increasingly apparent. Clarity of concept and consistency of
106 nomenclature are key trademarks of a research field. These features facilitate effective
107 transdisciplinary communication, education, and ultimately further discovery. The
108 chemiosmotic theory establishes the mechanism of energy transformation and coupling in
109 oxidative phosphorylation. The unifying concept of the protonmotive force provides the
110 framework for developing a consistent theoretical foundation of mitochondrial physiology and
111 bioenergetics. We follow IUPAC guidelines on terminology in physical chemistry, extended
112 by considerations on open systems and irreversible thermodynamics. The concept-driven
113 constructive terminology incorporates the meaning of each quantity and aligns concepts and
114 symbols to the nomenclature of classical bioenergetics. In the frame of COST Action
115 MitoEAGLE open to global bottom-up input, we endeavour to provide a balanced view on
116 mitochondrial respiratory control and a critical discussion on reporting data of mitochondrial
117 respiration in terms of metabolic flows and fluxes. Uniform standards for evaluation of
118 respiratory states and rates will ultimately support the development of databases of
119 mitochondrial respiratory function in species, tissues, and cells.

120

121 *Keywords:* Mitochondrial respiratory control, coupling control, mitochondrial
122 preparations, protonmotive force, uncoupling, oxidative phosphorylation, OXPHOS,
123 efficiency, electron transfer, ET; proton leak, LEAK, residual oxygen consumption, ROX, State
124 2, State 3, State 4, normalization, flow, flux, O₂

125

126

127

128 **Executive summary**

129

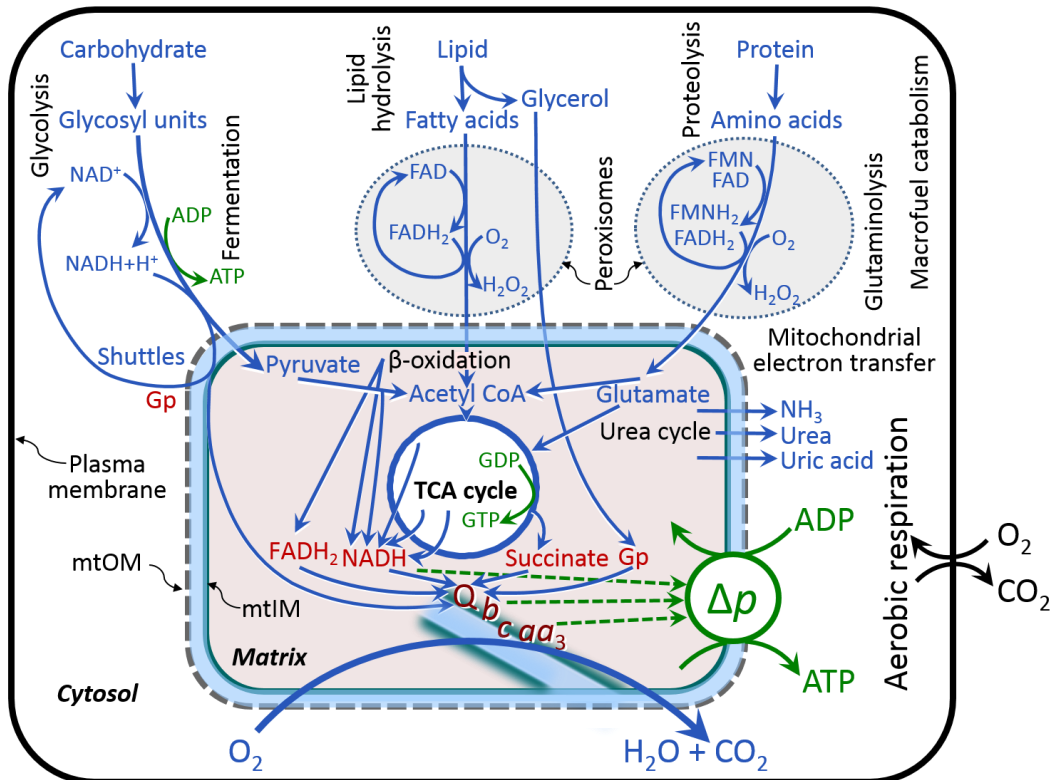
130 1. In view of broad implications on health care, mitochondrial researchers face an
131 increasing responsibility to disseminate their fundamental knowledge and novel
132 discoveries to a wide range of stakeholders and scientists beyond the group of
133 specialists. This requires implementation of a commonly accepted terminology
134 within the discipline and standardization in the translational context. Authors,
135 reviewers, journal editors, and lecturers are challenged to collaborate with the aim
136 to harmonize the nomenclature in the growing field of mitochondrial physiology
137 and bioenergetics.

138 2. Aerobic energy metabolism in mitochondria of most eukaryotic cells depends on the
139 coupling of phosphorylation ($\text{ADP} \rightarrow \text{ATP}$) to O₂ flux in catabolic reactions. In the
140 process of oxidative phosphorylation, coupling is mediated by translocation of
141 protons through respiratory proton pumps operating across the inner mitochondrial
142 membrane and generating or utilizing the protonmotive force measured between
143 the mitochondrial matrix and intermembrane compartment. Compartmental
144 coupling distinguishes vectorial oxidative phosphorylation from fermentation as the
145 counterpart of cellular core energy metabolism (**Figure 1**).

146 3. To exclude fermentation and other cytosolic interactions from exerting an effect on
147 mitochondrial metabolism, the barrier function of the plasma membrane must be
148 disrupted. Selective removal or permeabilization of the plasma membrane yields
149 mitochondrial preparations—including isolated mitochondria, tissue and cellular
150 preparations—with structural and functional integrity. Then extra-mitochondrial
151 concentrations of fuel substrates transported into the mitochondrial matrix, ADP,
152 ATP, inorganic phosphate, and cations including H⁺ can be controlled to determine
153 mitochondrial function under a set of conditions defined as coupling control states.

154
155
156
157

A concept-driven terminology of bioenergetics incorporates in its terms and symbols explicit information on the nature of respiratory states that makes the technical terms readily recognized and easy to understand.



158

159 **Figure 1. Mitochondrial respiration in the framework of cellular catabolism**

160 Mitochondrial respiration is the utilization of fuel substrates, which are the products of extra-
161 mitochondrial catabolism of macrofuels or are taken up by the cell as small molecules, for
162 electron transfer to O_2 as the electron acceptor. Many fuel substrates are catabolized to acetyl-
163 CoA or glutamate, and further electron transfer reduces nicotinamide adenine dinucleotide to
164 NADH or flavin adenine dinucleotide to $FADH_2$. In aerobic respiration, electron transfer is
165 coupled to the phosphorylation of ADP to ATP, with energy transformation mediated by the
166 protonmotive force, Δp . Anabolic reactions are tightly integrated with catabolism, both by ATP
167 as the intermediary energy currency and by small organic precursor molecules as building
168 blocks for biosynthesis (not shown). Glycolysis involves substrate-level phosphorylation of
169 ADP to ATP in fermentation without utilization of O_2 . In contrast, extra-mitochondrial
170 oxidation of fatty acids and amino acids proceeds partially in peroxisomes without coupling to
171 ATP production: acyl-CoA oxidase catalyzes the oxidation of $FADH_2$ with electron transfer to
172 O_2 ; amino acid oxidases oxidize flavin mononucleotide $FMNH_2$ or $FADH_2$. Coenzyme Q, Q,
173 and the cytochromes b , c , and aa_3 are redox systems of the mitochondrial inner membrane,
174 mtIM. Dashed arrows indicate the connection between the redox proton pumps (respiratory
175 Complexes CI, CIII and CIV) and the transmembrane Δp . Mitochondrial outer membrane,
176 mtOM; glycerol-3-phosphate, Gp; tricarboxylic acid cycle, TCA cycle.

177

178 4. Mitochondrial coupling states are defined according to the control of respiratory oxygen
179 flux by the protonmotive force. Capacities of oxidative phosphorylation and
180 electron transfer are measured at kinetically saturating concentrations of fuel
181 substrates, ADP and inorganic phosphate, or at optimal uncoupler concentrations,
182 respectively. Respiratory capacities are a measure of the upper bound of the rates
183 of respiration, providing reference values for the diagnosis of health and disease,

- 184 and for evaluation of the effects of **E**volutionary background, **A**ge, **G**ender and sex,
 185 **L**ifestyle and **E**nvironment (EAGLE).
- 186 5. Some degree of uncoupling is a characteristic of energy-transformations across
 187 membranes. Uncoupling is caused by a variety of physiological, pathological,
 188 toxicological, pharmacological and environmental conditions that exert an
 189 influence not only on the proton leak and cation cycling, but also on proton slip
 190 within the proton pumps and the structural integrity of the mitochondria. A more
 191 loosely coupled state is induced by stimulation of mitochondrial superoxide
 192 formation and the bypass of proton pumps. In addition, uncoupling by application
 193 of protonophores represents an experimental intervention for the transition from a
 194 well-coupled to the noncoupled state of mitochondrial respiration.
 - 195 6. Respiratory oxygen consumption rates have to be carefully normalized to enable meta-
 196 analytic studies beyond the specific question of a particular experiment. Therefore,
 197 all raw data should be published in a supplemental table or open access data
 198 repository. Normalization of rates for the volume of the experimental chamber (the
 199 measuring system) is distinguished from normalization for (1) the volume or mass
 200 of the experimental sample, (2) the number of objects (cells, organisms), and (3)
 201 the concentration of mitochondrial markers in the chamber.
 - 202 7. The consistent use of terms and symbols will facilitate transdisciplinary communication
 203 and support further developments of a database on bioenergetics and mitochondrial
 204 physiology. The present considerations are focused on studies with mitochondrial
 205 preparations. These will be extended in a series of reports on pathway control of
 206 mitochondrial respiration, the protonmotive force, respiratory states in intact cells,
 207 and harmonization of experimental procedures.

212 **Box 1: In brief – Mitochondria and Bioblasts**

214 **Mitochondria** are the oxygen-consuming electrochemical generators evolved from
 215 endosymbiotic bacteria (Margulis 1970; Lane 2005). They were described by Richard Altmann
 216 (1894) as ‘bioblasts’, which include not only the mitochondria as presently defined, but also
 217 symbiotic and free-living bacteria. The word ‘mitochondria’ (Greek mitos: thread; chondros:
 218 granule) was introduced by Carl Benda (1898).

219 Mitochondria are dynamic networks contained within eukaryotic cells morphologically
 220 characterized by a double membrane. The mitochondrial inner membrane (mtIM) shows
 221 dynamic tubular to disk-shaped cristae that separate the mitochondrial matrix, *i.e.*, the
 222 negatively charged internal mitochondrial compartment, from the intermembrane space; the
 223 latter being positively charged and enclosed by the mitochondrial outer membrane (mtOM).
 224 The mtIM contains the non-bilayer phospholipid cardiolipin, which is not present in any other
 225 eukaryotic cellular membrane. Cardiolipin promotes the formation of respiratory
 226 supercomplexes (SC I_nIII_nIV_n), which are supramolecular assemblies based upon specific,
 227 though dynamic interactions between individual respiratory complexes (Greggio *et al.* 2017;
 228 Lenaz *et al.* 2017). Membrane fluidity exerts an influence on functional properties of proteins
 229 incorporated in the membranes (Waczulikova *et al.* 2007). In addition to mitochondrial
 230 movement along microtubules, mitochondrial morphology can change in response to energy
 231 requirements of the cell via processes known as fusion and fission, through which mitochondria
 232 communicate within a network, and in response to intracellular stress factors causing swelling
 233 and ultimately permeability transition.

234 Mitochondria are the structural and functional elements of cell respiration. Mitochondrial
235 respiration is the reduction of oxygen by electron transfer coupled to electrochemical proton
236 translocation across the mtIM. In the process of oxidative phosphorylation (OXPHOS), the
237 catabolic reaction of oxygen consumption is electrochemically coupled to the transformation of
238 energy in the form of adenosine triphosphate (ATP; Mitchell 1961, 2011). Mitochondria are the
239 powerhouses of the cell which contain the machinery of the OXPHOS-pathways, including
240 transmembrane respiratory complexes (proton pumps with FMN, Fe-S and cytochrome *b*, *c*,
241 *aa₃* redox systems); alternative dehydrogenases and oxidases; the coenzyme ubiquinone (Q);
242 F-ATPase or ATP synthase; the enzymes of the tricarboxylic acid cycle, fatty acid and
243 aminoacid oxidation; transporters of ions, metabolites and co-factors; and mitochondrial
244 kinases related to energy transfer pathways. The mitochondrial proteome comprises over 1,200
245 proteins (Calvo *et al.* 2015; 2017), mostly encoded by nuclear DNA (nDNA), with a variety of
246 functions, many of which are relatively well known (*e.g.*, proteins regulating mitochondrial
247 biogenesis or apoptosis), while others are still under investigation, or need to be identified (*e.g.*,
248 alanine transporter).

249 There is a constant crosstalk between mitochondria and the other cellular components.
250 The crosstalk between mitochondria and endoplasmic reticulum is involved in the regulation of
251 calcium homeostasis, cell division, autophagy, differentiation, and anti-viral signaling (Murley
252 and Nunnari 2016). Mitochondria contribute to the formation of peroxisomes, which are hybrids
253 of mitochondrial and ER-derived precursors (Sugiura *et al.* 2017). Cellular mitochondrial
254 homeostasis (mitostasis) is maintained through regulation at both the transcriptional and post-
255 translational level. Cell signalling modules contribute to homeostatic regulation throughout the
256 cell cycle or even cell death by activating proteostatic modules (*e.g.*, the ubiquitin-proteasome
257 and autophagy-lysosome pathways) and genome stability modules in response to varying
258 energy demands and stress cues (Quiros *et al.* 2016).

259 Mitochondria typically maintain several copies of their own genome known as
260 mitochondrial DNA (mtDNA; hundred to thousands per cell; Cummins 1998), which is
261 maternally inherited. Biparental mitochondrial inheritance is documented in mammals, birds,
262 fish, reptiles and invertebrate groups, and is even the norm in bivalves (Breton *et al.* 2007;
263 White *et al.* 2008). mtDNA is compact (16.5 kB in humans) and encodes 13 protein subunits
264 of the transmembrane respiratory Complexes CI, CIII, CIV and F-ATPase, 22 tRNAs, and two
265 RNAs. Additional gene content has been suggested to include microRNAs, piRNA,
266 smithRNAs, repeat associated RNA, and even additional proteins (Duarte *et al.* 2014; Lee *et al.*
267 *et al.* 2015; Cobb *et al.* 2016). The mitochondrial genome requires nuclear-encoded
268 mitochondrially targeted proteins for its maintenance and expression (Rackham *et al.* 2012).

269 Mitochondrial dysfunction is associated with a wide variety of genetic and degenerative
270 diseases. Robust mitochondrial function is supported by physical exercise and caloric balance,
271 and is central for sustained metabolic health throughout life. Therefore, a more consistent
272 presentation of mitochondrial physiology will improve our understanding of the etiology of
273 disease, the diagnostic repertoire of mitochondrial medicine, with a focus on protective
274 medicine, lifestyle and healthy aging.

275 Abbreviation: mt, as generally used in mtDNA. Mitochondrion is singular and
276 mitochondria is plural.

277 ‘For the physiologist, mitochondria afforded the first opportunity for an experimental
278 approach to structure-function relationships, in particular those involved in active transport,
279 vectorial metabolism, and metabolic control mechanisms on a subcellular level’ (Ernster and
280 Schatz 1981).

281

282

283

284

285 1. Introduction

286

287 Mitochondria are the powerhouses of the cell with numerous physiological, molecular,
288 and genetic functions (**Box 1**). Every study of mitochondrial health and disease is faced with
289 **E**volution, **A**ge, **G**ender and sex, **L**ifestyle, and **E**nvironment (EAGLE) as essential background
290 conditions intrinsic to the individual patient or subject, cohort, species, tissue and to some extent
291 even cell line. As a large and coordinated group of laboratories and researchers, the mission of
292 the global MitoEAGLE Network is to generate the necessary scale, type, and quality of
293 consistent data sets and conditions to address this intrinsic complexity. Harmonization of
294 experimental protocols and implementation of a quality control and data management system
295 are required to interrelate results gathered across a spectrum of studies and to generate a
296 rigorously monitored database focused on mitochondrial respiratory function. In this way,
297 researchers within the same and across different disciplines can compare findings across
298 traditions and generations to clearly defined and accepted international standards.

299 Reliability and comparability of quantitative results depend on the accuracy of
300 measurements under strictly-defined conditions. A conceptual framework is required to warrant
301 meaningful interpretation and comparability of experimental outcomes carried out by research
302 groups at different institutes. With an emphasis on quality of research, collected data can be
303 useful far beyond the specific question of a particular experiment. Enabling meta-analytic
304 studies is the most economic way of providing robust answers to biological questions (Cooper
305 *et al.* 2009). Vague or ambiguous jargon can lead to confusion and may relegate valuable
306 signals to wasteful noise. For this reason, measured values must be expressed in standard units
307 for each parameter used to define mitochondrial respiratory function. Harmonization of
308 nomenclature and definition of technical terms are essential to improve the awareness of the
309 intricate meaning of current and past scientific vocabulary, for documentation and integration
310 into databases in general, and quantitative modelling in particular (Beard 2005). The focus on
311 coupling states and fluxes through metabolic pathways of aerobic energy transformation in
312 mitochondrial preparations is a first step in the attempt to generate a conceptually-oriented
313 nomenclature in bioenergetics and mitochondrial physiology. Coupling states of intact cells,
314 the protonmotive force, and respiratory control by fuel substrates and specific inhibitors of
315 respiratory enzymes will be reviewed in subsequent communications.

316

317

318 2. Oxidative phosphorylation and coupling states in mitochondrial preparations

319 *‘Every professional group develops its own technical jargon for talking about matters of*
320 *critical concern ... People who know a word can share that idea with other members of*
321 *their group, and a shared vocabulary is part of the glue that holds people together and*
322 *allows them to create a shared culture’ (Miller 1991).*

323

324 **Mitochondrial preparations** are defined as either isolated mitochondria, or tissue and
325 cellular preparations in which the barrier function of the plasma membrane is disrupted. Since
326 this entails the loss of cell viability, mitochondrial preparations are not studied *in vivo*. In
327 contrast to isolated mitochondria and tissue homogenate preparations, mitochondria in
328 permeabilized tissues and cells are *in situ* relative to the plasma membrane. The plasma
329 membrane separates the intracellular compartment including the cytosol, nucleus, and
330 organelles from the environment of the cell. The plasma membrane consists of a lipid bilayer
331 with embedded proteins and attached organic molecules that collectively control the selective
332 permeability of ions, organic molecules, and particles across the cell boundary. The intact
333 plasma membrane prevents the passage of many water-soluble mitochondrial substrates and
334 inorganic ions—such as succinate, adenosine diphosphate (ADP) and inorganic phosphate (P_i),
335 that must be controlled at kinetically-saturating concentrations for the analysis of respiratory

336 capacities; this limits the scope of investigations into mitochondrial respiratory function in
337 intact cells.

338 The cholesterol content of the plasma membrane is high compared to mitochondrial
339 membranes. Therefore, mild detergents—such as digitonin and saponin—can be applied to
340 selectively permeabilize the plasma membrane by interaction with cholesterol and allow free
341 exchange of organic molecules and inorganic ions between the cytosol and the immediate cell
342 environment, while maintaining the integrity and localization of organelles, cytoskeleton, and
343 the nucleus. Application of optimum concentrations of permeabilization agents (mild detergents
344 or toxins) leads to washout of cytosolic marker enzymes—such as lactate dehydrogenase—and
345 results in the complete loss of cell viability, tested by nuclear staining using membrane-
346 impermeable dyes, while mitochondrial function remains intact. Respiration of isolated
347 mitochondria remains unaltered after the addition of low concentrations of digitonin or saponin.
348 In addition to mechanical cell disruption during homogenization of tissue, permeabilization
349 agents may be applied to ensure permeabilization of all cells. Suspensions of cells
350 permeabilized in the respiration chamber and crude tissue homogenates contain all components
351 of the cell at highly dilute concentrations. All mitochondria are retained in chemically-
352 permeabilized mitochondrial preparations and crude tissue homogenates. In the preparation of
353 isolated mitochondria, the cells or tissues are homogenized, and the mitochondria are separated
354 from other cell fractions and purified by differential centrifugation, entailing the loss of a
355 fraction of the total mitochondrial content. Typical mitochondrial recovery ranges from 30% to
356 80%. Maximization of the purity of isolated mitochondria may compromise not only the
357 mitochondrial yield but also the structural and functional integrity. Therefore, protocols to
358 isolate mitochondria need to be optimized according to each study. The term mitochondrial
359 preparation does not include further fractionation of mitochondrial components, neither
360 submitochondrial particles.

361

362 *2.1. Respiratory control and coupling*

363

364 Respiratory coupling control states are established in studies of mitochondrial
365 preparations to obtain reference values for various output variables. Physiological conditions *in*
366 *vivo* deviate from these experimentally obtained states. Since kinetically-saturating
367 concentrations, *e.g.*, of ADP or oxygen (O₂; dioxygen), may not apply to physiological
368 intracellular conditions, relevant information is obtained in studies of kinetic responses to
369 variations in [ADP] or [O₂] in the range between kinetically-saturating concentrations and
370 anoxia (Gnaiger 2001).

371 **The steady-state:** Mitochondria represent a thermodynamically open system in non-
372 equilibrium states of biochemical energy transformation. State variables (protonmotive force;
373 redox states) and metabolic *rates* (fluxes) are measured in defined mitochondrial respiratory
374 *states*. Steady-states can be obtained only in open systems, in which changes by *internal*
375 transformations, *e.g.*, O₂ consumption, are instantaneously compensated for by *external* fluxes,
376 *e.g.*, O₂ supply, preventing a change of O₂ concentration in the system (Gnaiger 1993b).
377 Mitochondrial respiratory states monitored in closed systems satisfy the criteria of pseudo-
378 steady states for limited periods of time, when changes in the system (concentrations of O₂, fuel
379 substrates, ADP, P_i, H⁺) do not exert significant effects on metabolic fluxes (respiration,
380 phosphorylation). Such pseudo-steady states require respiratory media with sufficient buffering
381 capacity and substrates maintained at kinetically-saturating concentrations, and thus depend on
382 the kinetics of the processes under investigation.

383 **Specification of biochemical dose:** Substrates, uncouplers, inhibitors, and other
384 chemical reagents are titrated to dissect mitochondrial function. Nominal concentrations of
385 these substances are usually reported as initial amount of substance concentration [mol·L⁻¹] in
386 the incubation medium. When aiming at the measurement of kinetically saturated processes—

387 such as OXPHOS-capacities, the concentrations for substrates can be chosen according to the
 388 apparent equilibrium constant, K_m' . In the case of hyperbolic kinetics, only 80% of maximum
 389 respiratory capacity is obtained at a substrate concentration of four times the K_m' , whereas
 390 substrate concentrations of 5, 9, 19 and 49 times the K_m' are theoretically required for reaching
 391 83%, 90%, 95% or 98% of the maximal rate (Gnaiger 2001). Other reagents are chosen to
 392 inhibit or alter some processes. The amount of these chemicals in an experimental incubation
 393 is selected to maximize effect, avoiding unacceptable off-target consequences that would
 394 adversely affect the data being sought. Specifying the amount of substance in an incubation as
 395 nominal concentration in the aqueous incubation medium can be ambiguous (Doskey *et al.*
 396 2015), particularly for lipophilic substances (oligomycin, uncouplers, permeabilization agents)
 397 or cations (TPP⁺; fluorescent dyes such as safranin, TMRM), which accumulate in biological
 398 membranes or in the mitochondrial matrix. For example, a dose of digitonin of 8 fmol·cell⁻¹ (10
 399 pg·cell⁻¹; 10 µg·10⁻⁶ cells) is optimal for permeabilization of endothelial cells, and the
 400 concentration in the incubation medium has to be adjusted according to the cell density applied
 401 (Doerrier *et al.* 2018).

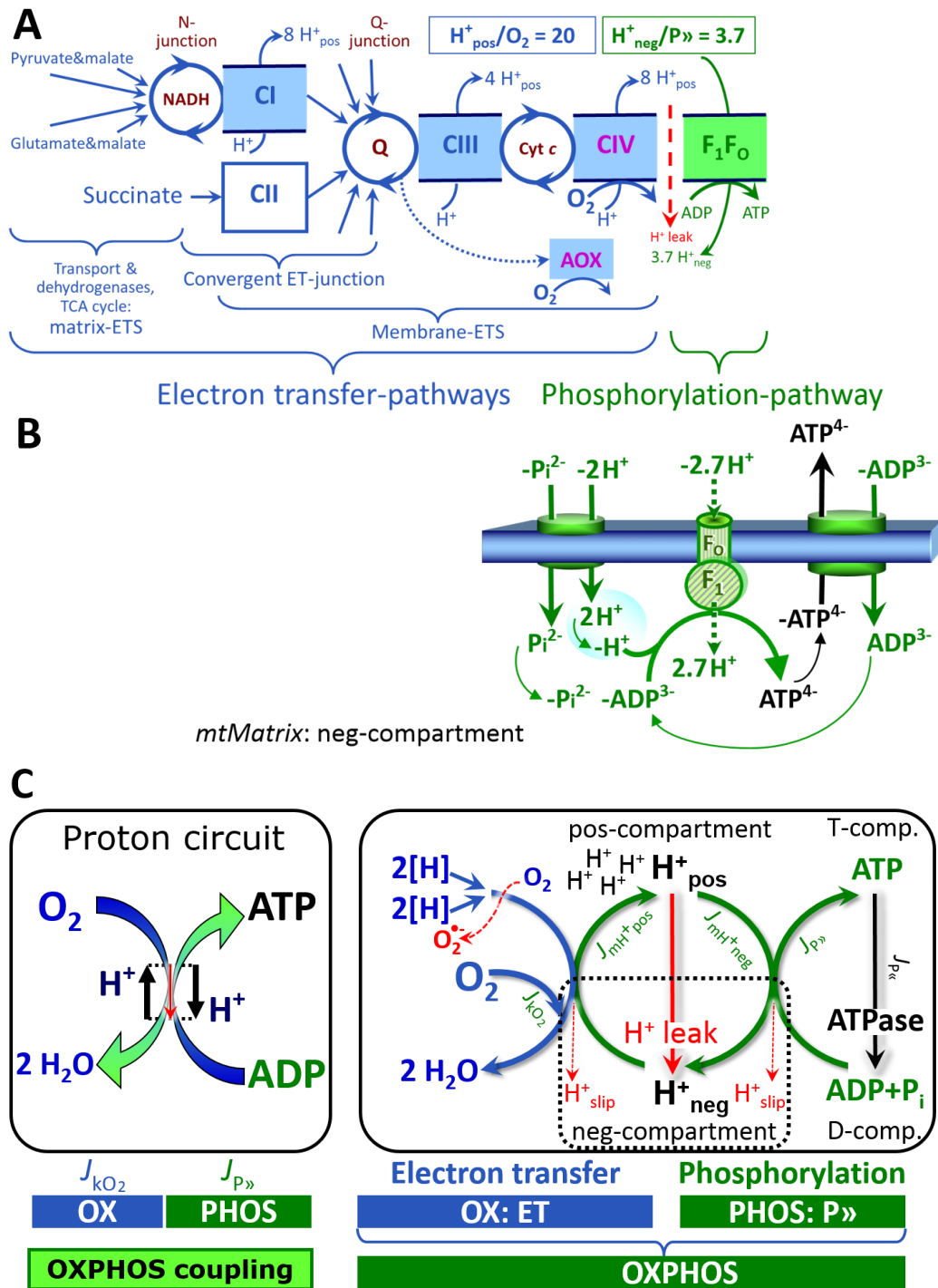
402 Generally, dose/exposure can be specified per unit of biological sample, *i.e.*, (nominal
 403 moles of xenobiotic)/(number of cells) [mol·cell⁻¹] or, as appropriate, per mass of biological
 404 sample [mol·kg⁻¹]. This approach to specification of dose/exposure provides a scalable
 405 parameter that can be used to design experiments, help interpret a wide variety of experimental
 406 results, and provide absolute information that allows researchers worldwide to make the most
 407 use of published data (Doskey *et al.* 2015).

408 **Phosphorylation, P \gg , and P \gg /O $_2$ ratio:** *Phosphorylation* in the context of OXPHOS is
 409 defined as phosphorylation of ADP by P_i to form ATP. On the other hand, the term
 410 phosphorylation is used generally in many contexts, *e.g.*, protein phosphorylation. This justifies
 411 consideration of a symbol more discriminating and specific than P as used in the P/O ratio
 412 (phosphate to atomic oxygen ratio), where P indicates phosphorylation of ADP to ATP or GDP
 413 to GTP (**Figure 1**). We propose the symbol P \gg for the endergonic (uphill) direction of
 414 phosphorylation ADP→ATP, and likewise the symbol P \ll for the corresponding exergonic
 415 (downhill) hydrolysis ATP→ADP (**Figure 2**). P \gg refers mainly to electrontransfer
 416 phosphorylation but may also involve substrate-level phosphorylation as part of the
 417 tricarboxylic acid (TCA) cycle (succinyl-CoA ligase; phosphoglycerate kinase) and
 418 phosphorylation of ADP catalyzed by pyruvate kinase, and of GDP phosphorylated by
 419 phosphoenolpyruvate carboxykinase. Transphosphorylation is performed by adenylate kinase,
 420 creatine kinase, hexokinase and nucleoside diphosphate kinase. In isolated mammalian
 421 mitochondria, ATP production catalyzed by adenylate kinase (2 ADP ↔ ATP + AMP) proceeds
 422 without fuel substrates in the presence of ADP (Komlódi and Tretter 2017). Kinase cycles are
 423 involved in intracellular energy transfer and signal transduction for regulation of energy flux.

424 The P \gg /O $_2$ ratio (P \gg /4 e⁻) is two times the 'P/O' ratio (P \gg /2 e⁻) of classical bioenergetics.
 425 P \gg /O $_2$ is a generalized symbol, not specific for determination of P_i consumption (P_i/O $_2$ flux
 426 ratio), ADP depletion (ADP/O $_2$ flux ratio), or ATP production (ATP/O $_2$ flux ratio). The
 427 mechanistic P \gg /O $_2$ ratio—or P \gg /O $_2$ stoichiometry—is calculated from the proton-to-O $_2$ and
 428 proton-to-phosphorylation coupling stoichiometries (**Figure 2A**):
 429

$$430 \quad P\gg/O_2 = \frac{H_{pos}^+/O_2}{H_{neg}^+/P\gg} \quad (1)$$

431
 432 The H⁺_{pos}/O $_2$ *coupling stoichiometry* (referring to the full 4 electron reduction of O $_2$) depends
 433 on the ET-pathway control state which defines the relative involvement of the three coupling
 434 sites (CI, CIII and CIV) in the catabolic pathway of electrons to O $_2$. This varies with: (1) a
 435 bypass of CI by single or multiple electron input into the Q-junction; and (2) a bypass of CIV
 436 by involvement of alternative oxidases, AOX, which are not expressed in mammalian
 437 mitochondria.



438 **Figure 2. Oxidative phosphorylation (OXPHOS)**
 439 (A) The mitochondrial electron transfer system (ETS) is fuelled by diffusion and transport of
 440 substrates across the mitochondrial outer and inner membrane and consists of the matrix-ETS
 441 and membrane-ETS. ET-pathways are coupled to the phosphorylation-pathway. ET-pathways
 442 converge at the N-junction and Q-junction. Additional arrows indicate electron entry into the
 443 Q-junction through electron transferring flavoprotein, glycerophosphate dehydrogenase,
 444 dihydro-orotate dehydrogenase, choline dehydrogenase, and sulfide-ubiquinone
 445 oxidoreductase. The dotted arrow indicates the branched pathway of oxygen consumption by
 446 alternative quinol oxidase (AOX). The H^+_{pos}/O_2 ratio is the outward proton flux from the matrix
 447 space to the positively (pos) charged vesicular compartment, divided by catabolic O_2 flux in the
 448 NADH-pathway. The $H^+_{neg}/P \gg$ ratio is the inward proton flux from the inter-membrane space

449 to the negatively (neg) charged matrix space, divided by the flux of phosphorylation of ADP to
 450 ATP. These are not fixed stoichiometries due to ion leaks and proton slip.

451 **(B)** Phosphorylation-pathway catalyzed by the proton pump F_1F_0 -ATPase (F-ATPase, ATP
 452 synthase), adenine nucleotide translocase, and inorganic phosphate transporter. The H^+_{neg}/P_{\gg}
 453 stoichiometry is the sum of the coupling stoichiometry in the F-ATPase reaction ($-2.7 H^+_{pos}$
 454 from the positive intermembrane space, $2.7 H^+_{neg}$ to the matrix, *i.e.*, the negative compartment)
 455 and the proton balance in the translocation of ADP^{3-} , ATP^{4-} and P_i^{2-} .

456 **(C)** The proton circuit and coupling in OXPHOS. $2[H]$ indicates the reduced hydrogen
 457 equivalents of fuel substrates of the catabolic reaction k with oxygen. O_2 flux, J_{kO_2} , through the
 458 catabolic ET-pathway, is coupled to flux through the phosphorylation-pathway of ADP to ATP,
 459 $J_{P_{\gg}}$. The redox proton pumps of the ET-pathway drive proton flux into the positive (pos)
 460 compartment, J_{mH+pos} , generating the output protonmotive force (motive, subscript m). F-
 461 ATPase is coupled to inward proton current into the negative (neg) compartment, J_{mH+neg} , to
 462 phosphorylate $ADP+P_i$ to ATP. The system is defined by the boundaries (full black line) and is
 463 not a black box, but is analysed as a compartmental system. The negative compartment (neg-
 464 compartment, enclosed by the dotted line) is the matrix space, separated by the mtIM from the
 465 positive compartment (pos-compartment). $ADP+P_i$ and ATP are the substrate- and product-
 466 compartments (scalar ADP and ATP compartments, D-comp. and T-comp.), respectively. At
 467 steady-state proton turnover, $J_{\infty H+}$, and ATP turnover, $J_{\infty P}$, maintain concentrations constant,
 468 when $J_{mH+\infty} = J_{mH+pos} = J_{mH+neg}$, and $J_{P\infty} = J_{P_{\gg}} = J_{P_{\ll}}$. Modified from (A) Lemieux *et al.* (2017)
 469 and (B,C) Gnaiger (2014).

470

471 H^+_{pos}/O_2 is 12 in the ET-pathways involving CIII and CIV as proton pumps, increasing to
 472 20 for the NADH-pathway (**Figure 2A**), but a general consensus on H^+_{pos}/O_2 stoichiometries
 473 remains to be reached (Hinkle 2005; Wikström and Hummer 2012; Sazanov 2015). The
 474 H^+_{neg}/P_{\gg} coupling stoichiometry (3.7; **Figure 2A**) is the sum of $2.7 H^+_{neg}$ required by the F-
 475 ATPase of vertebrate and most invertebrate species (Watt *et al.* 2010) and the proton balance
 476 in the translocation of ADP, ATP and P_i (**Figure 2B**). Taken together, the mechanistic P_{\gg}/O_2
 477 ratio is calculated at 5.4 and 3.3 for NADH- and succinate-linked respiration, respectively (Eq.
 478 1). The corresponding classical P_{\gg}/O ratios (referring to the 2 electron reduction of $0.5 O_2$) are
 479 2.7 and 1.6 (Watt *et al.* 2010), in agreement with the measured P_{\gg}/O ratio for succinate of 1.58
 480 ± 0.02 (Gnaiger *et al.* 2000).

481 The effective P_{\gg}/O_2 flux ratio ($Y_{P_{\gg}/O_2} = J_{P_{\gg}}/J_{kO_2}$) is diminished relative to the mechanistic
 482 P_{\gg}/O_2 ratio by intrinsic and extrinsic uncoupling and dyscoupling (**Figure 3**). Such generalized
 483 uncoupling is different from switching to mitochondrial pathways that involve fewer than three
 484 proton pumps ('coupling sites': Complexes CI, CIII and CIV), bypassing CI through multiple
 485 electron entries into the Q-junction, or CIII and CIV through AOX (**Figure 2**). Reprogramming
 486 of mitochondrial pathways may be considered as a switch of gears (changing the stoichiometry)
 487 rather than uncoupling (loosening the stoichiometry). In addition, Y_{P_{\gg}/O_2} depends on several
 488 experimental conditions of flux control, increasing as a hyperbolic function of $[ADP]$ to a
 489 maximum value (Gnaiger 2001).

490 **Control and regulation:** The terms metabolic *control* and *regulation* are frequently used
 491 synonymously, but are distinguished in metabolic control analysis: 'We could understand the
 492 regulation as the mechanism that occurs when a system maintains some variable constant over
 493 time, in spite of fluctuations in external conditions (homeostasis of the internal state). On the
 494 other hand, metabolic control is the power to change the state of the metabolism in response to
 495 an external signal' (Fell 1997). Respiratory control may be induced by experimental control
 496 signals that *exert* an influence on: (1) ATP demand and ADP phosphorylation-rate; (2) fuel
 497 substrate composition, pathway competition; (3) available amounts of substrates and O_2 , *e.g.*,
 498 starvation and hypoxia; (4) the protonmotive force, redox states, flux-force relationships,
 499 coupling and efficiency; (5) Ca^{2+} and other ions including H^+ ; (6) inhibitors, *e.g.*, nitric oxide

500 or intermediary metabolites such as oxaloacetate; (7) signalling pathways and regulatory
 501 proteins, *e.g.*, insulin resistance, transcription factor hypoxia inducible factor 1. *Mechanisms* of
 502 respiratory control and regulation include adjustments of: (1) enzyme activities by allosteric
 503 mechanisms and phosphorylation; (2) enzyme content, concentrations of cofactors and
 504 conserved moieties—such as adenylates, nicotinamide adenine dinucleotide [NAD⁺/NADH],
 505 coenzyme Q, cytochrome *c*; (3) metabolic channeling by supercomplexes; and (4)
 506 mitochondrial density (enzyme concentrations and membrane area) and morphology (cristae
 507 folding, fission and fusion). Mitochondria are targeted directly by hormones, thereby affecting
 508 their energy metabolism (Lee *et al.* 2013; Gerö and Szabo 2016; Price and Dai 2016; Moreno
 509 *et al.* 2017). Evolutionary or acquired differences in the genetic and epigenetic basis of
 510 mitochondrial function (or dysfunction) between subjects and gene therapy; age; gender,
 511 biological sex, and hormone concentrations; life style including exercise and nutrition; and
 512 environmental issues including thermal, atmospheric, toxicological and pharmacological
 513 factors, exert an influence on all control mechanisms listed above. For reviews, see Brown
 514 1992; Gnaiger 1993a, 2009; 2014; Paradies *et al.* 2014; Morrow *et al.* 2017.

515 **Respiratory control and response:** Lack of control by a metabolic pathway, *e.g.*,
 516 phosphorylation-pathway, means that there will be no response to a variable activating it, *e.g.*,
 517 [ADP]. The reverse, however, is not true as the absence of a response to [ADP] does not exclude
 518 the phosphorylation-pathway from having some degree of control. The degree of control of a
 519 component of the OXPHOS-pathway on an output variable—such as O₂ flux, will in general
 520 be different from the degree of control on other outputs—such as phosphorylation-flux or
 521 proton leak flux. Therefore, it is necessary to be specific as to which input and output are under
 522 consideration (Fell 1997).

523 **Respiratory coupling control and ET-pathway control:** Respiratory control refers to
 524 the ability of mitochondria to adjust O₂ flux in response to external control signals by engaging
 525 various mechanisms of control and regulation. Respiratory control is monitored in a
 526 mitochondrial preparation under conditions defined as respiratory states. When
 527 phosphorylation of ADP to ATP is stimulated or depressed, an increase or decrease is observed
 528 in electron transfer measured as O₂ flux in respiratory coupling states of intact mitochondria
 529 ('controlled states' in the classical terminology of bioenergetics). Alternatively, coupling of
 530 electron transfer with phosphorylation is disengaged by uncouplers. These protonophores are
 531 weak lipid-soluble acids which disrupt the barrier function of the mtIM and thus shortcircuit
 532 the protonmotive system, functioning like a clutch in a mechanical system. The corresponding
 533 coupling control state is characterized by a high O₂ flux without control by P_» ('uncontrolled
 534 state').

535 ET-pathway control states are obtained in mitochondrial preparations by depletion of
 536 endogenous substrates and addition to the mitochondrial respiration medium of fuel substrates
 537 (2[H] in **Figure 2C**) and specific inhibitors, activating selected mitochondrial catabolic
 538 pathways, *k* (**Figure 2A**). Coupling control states and pathway control states are
 539 complementary, since mitochondrial preparations depend on an exogenous supply of pathway-
 540 specific fuel substrates and oxygen (Gnaiger 2014).

541 **Coupling:** In mitochondrial electron transfer, vectorial transmembrane proton flux is
 542 coupled through the redox proton pumps CI, CIII and CIV to the catabolic flux of scalar
 543 reactions, collectively measured as O₂ flux (**Figure 2**). Thus mitochondria are elements of
 544 energy transformation. Energy cannot be lost or produced in any internal process (First Law of
 545 thermodynamics). Open and closed systems can gain or lose energy only by external fluxes—
 546 by exchange with the environment. Energy is a conserved quantity. Therefore, energy can
 547 neither be produced by mitochondria, nor is there any internal process without energy
 548 conservation. Exergy is defined as the Gibbs energy ('free energy') with the potential to
 549 perform work under conditions of constant volume and pressure. *Coupling* is the interaction of
 550 an exergonic process (spontaneous, negative exergy change) with an endergonic process

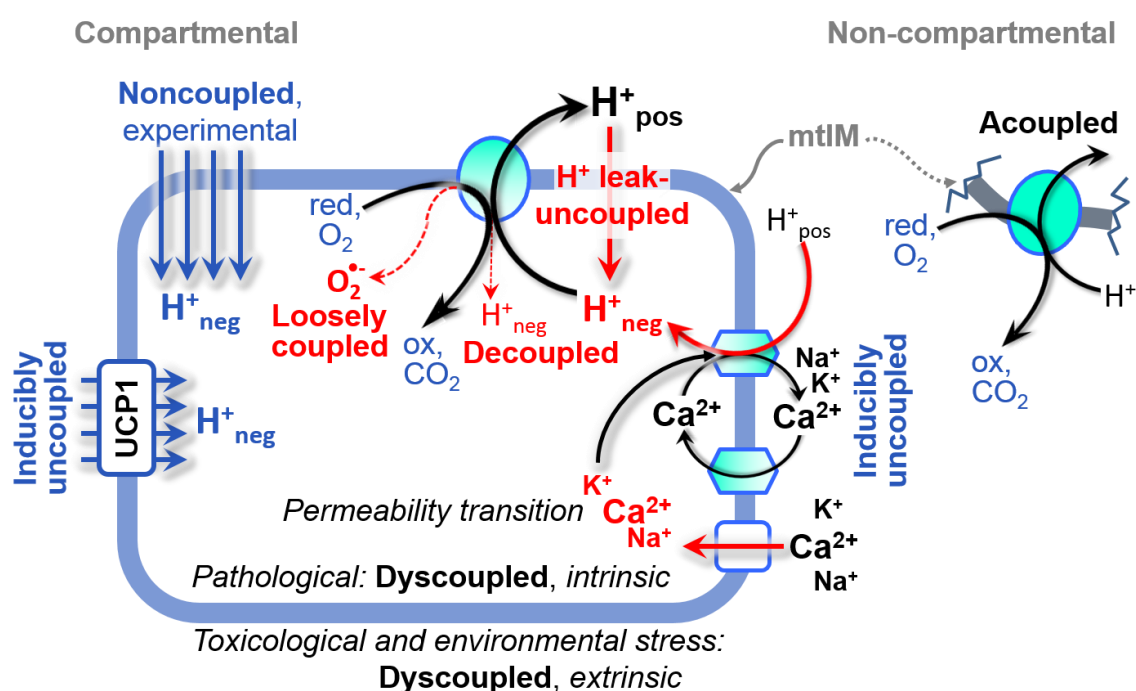
551 (positive exergy change) in energy transformations which conserve part of the exergy that
 552 would be irreversibly lost or dissipated in an uncoupled process.

553 **Uncoupling:** Uncoupling of mitochondrial respiration is a general term comprising
 554 diverse mechanisms:

- 555 1. Proton leak across the mtIM from the pos- to the neg-compartment (**Figure 2C**);
- 556 2. Cycling of other cations, strongly stimulated by permeability transition, or
 557 experimentally induced by valinomycin in the presence of K^+ ;
- 558 3. Proton slip in the redox proton pumps when protons are effectively not pumped (CI,
 559 CIII and CIV) or are not driving phosphorylation (F-ATPase);
- 560 4. Loss of vesicular (compartmental) integrity when electron transfer is acoupled;
- 561 5. Electron leak in the loosely coupled univalent reduction of O_2 to superoxide ($O_2^{\cdot-}$;
 562 superoxide anion radical).

563 Differences of terms—uncoupled vs. noncoupled—are easily overlooked, although they relate
 564 to different meanings of uncoupling (**Figure 3**).

565



566

567

568 **Figure 3. Mechanisms of respiratory uncoupling**

568 An intact mitochondrial inner membrane, mtIM, is required for vectorial, compartmental
 569 coupling. ‘Acoupled’ respiration is the consequence of structural disruption with catalytic
 570 activity of non-compartmental mitochondrial fragments. Inducibly uncoupled (activation of
 571 UCP1) and experimentally noncoupled respiration (titration of protonophores) stimulate
 572 respiration to maximum O_2 flux. H^+ leak-uncoupled, decoupled, and loosely coupled
 573 respiration are components of intrinsic uncoupling. Pathological dysfunction may affect all types of
 574 uncoupling, including permeability transition, causing intrinsically dyscoupled respiration.
 575 Similarly, toxicological and environmental stress factors can cause extrinsically dyscoupled
 576 respiration.

577

578 **2.2. Coupling states and respiratory rates**

579

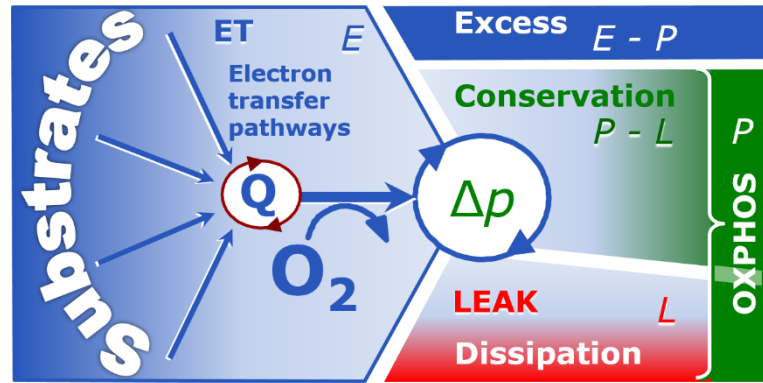
580 **Respiratory capacities in coupling control states:** To extend the classical nomenclature
 581 on mitochondrial coupling states (Section 2.3) by a concept-driven terminology that
 582 incorporates explicitly information on the meaning of respiratory states, the terminology must
 583 be general and not restricted to any particular experimental protocol or mitochondrial

584 preparation (Gnaiger 2009). Concept-driven nomenclature aims at mapping the *meaning and*
 585 *concept behind* the words and acronyms onto the *forms* of words and acronyms (Miller 1991).
 586 The focus of concept-driven nomenclature is primarily the conceptual ‘why’, along with
 587 clarification of the experimental ‘how’. Respiratory capacities delineate, comparable to channel
 588 capacity in information theory (Schneider 2006), the upper bound of the rate of respiration
 589 measured in defined coupling control states and electron transfer-pathway (ET-pathway) states
 590 (Figure 4).

591

592 **Figure 4. Four-compartment**
 593 **model of oxidative**
 594 **phosphorylation**

595 Respiratory states (ET,
 596 OXPHOS, LEAK; Table 1) and
 597 corresponding rates (E , P , L) are
 598 connected by the protonmotive
 599 force, Δp . ET-capacity, E (I), is
 600 partitioned into (2) dissipative
 601 LEAK-respiration, L , when the
 602 Gibbs energy change of catabolic



603 O_2 flux is irreversibly lost, (3) net OXPHOS-capacity, $P-L$, with partial conservation of the
 604 capacity to perform work, and (4) the excess capacity, $E-P$. Modified from Gnaiger (2014).

605

606 **Table 1. Coupling states and residual oxygen consumption in mitochondrial**
 607 **preparations in relation to respiration- and phosphorylation-flux, J_{kO_2} and $J_{P_{\gg}}$,**
 608 **and protonmotive force, Δp .** Coupling states are established at kinetically-saturating
 609 concentrations of fuel substrates and O_2 .

State	J_{kO_2}	$J_{P_{\gg}}$	Δp	Inducing factors	Limiting factors
LEAK	L ; low, cation leak-dependent respiration	0	max.	proton leak, slip, and cation cycling	$J_{P_{\gg}} = 0$: (1) without ADP, L_N ; (2) max. ATP/ADP ratio, L_T ; or (3) inhibition of the phosphorylation-pathway, L_{Omy}
OXPHOS	P ; high, ADP-stimulated respiration	max.	high	kinetically-saturating [ADP] and $[P_i]$	$J_{P_{\gg}}$ by phosphorylation-pathway; or J_{kO_2} by ET-capacity
ET	E ; max., noncoupled respiration	0	low	optimal external uncoupler concentration for max. $J_{O_2, E}$	J_{kO_2} by ET-capacity
ROX	R_{ox} ; min., residual O_2 consumption	0	0	$J_{O_2, Rox}$ in non-ET-pathway oxidation reactions	full inhibition of ET-pathway; or absence of fuel substrates

610

611 To provide a diagnostic reference for respiratory capacities of core energy metabolism,
 612 the capacity of *oxidative phosphorylation*, OXPHOS, is measured at kinetically-saturating
 613 concentrations of ADP and P_i . The *oxidative* ET-capacity reveals the limitation of OXPHOS-
 614 capacity mediated by the *phosphorylation*-pathway. The ET- and phosphorylation-pathways

615 comprise coupled segments of the OXPHOS-system. ET-capacity is measured as noncoupled
 616 respiration by application of *external uncouplers*. The contribution of *intrinsically uncoupled*
 617 O₂ consumption is studied by preventing the stimulation of phosphorylation either in the
 618 absence of ADP or by inhibition of the phosphorylation-pathway. The corresponding states are
 619 collectively classified as LEAK-states, when O₂ consumption compensates mainly for ion
 620 leaks, including the proton leak. Defined coupling states are induced by: (1) adding cation
 621 chelators such as EGTA, binding free Ca²⁺ and thus limiting cation cycling; (2) adding ADP
 622 and P_i; (3) inhibiting the phosphorylation-pathway; and (4) uncoupler titrations, while
 623 maintaining a defined ET-pathway state with constant fuel substrates and inhibitors of specific
 624 branches of the ET-pathway (**Figure 4**).

625
 626 The three coupling states, ET, LEAK and OXPHOS, are shown schematically with the
 627 corresponding respiratory rates, abbreviated as *E*, *L* and *P*, respectively (**Figure 4**). We
 628 distinguish metabolic *pathways* from metabolic *states* and the corresponding metabolic *rates*;
 629 for example: ET-pathways (**Figure 4**), ET-states (**Figure 5C**), and ET-capacities, *E*,
 630 respectively (**Table 1**). The protonmotive force is *high* in the OXPHOS-state when it drives
 631 phosphorylation, *maximum* in the LEAK-state of coupled mitochondria, driven by LEAK-
 632 respiration at a minimum back flux of cations to the matrix side, and *very low* in the ET-state
 633 when uncouplers short-circuit the proton cycle (**Table 1**).

649 **LEAK-state (Figure 5A):**
 650 The LEAK-state is defined as a state of mitochondrial respiration when O₂ flux mainly
 651 compensates for ion leaks in the absence of ATP synthesis, at kinetically-saturating
 652 concentrations of O₂ and respiratory fuel substrates. LEAK-respiration is measured to
 653 obtain an estimate of *intrinsic uncoupling* without addition of an experimental uncoupler: (1)
 654 in the absence of adenylates, *i.e.*, AMP, ADP and ATP; (2) after depletion of ADP at a maximum
 655 ATP/ADP ratio; or (3) after

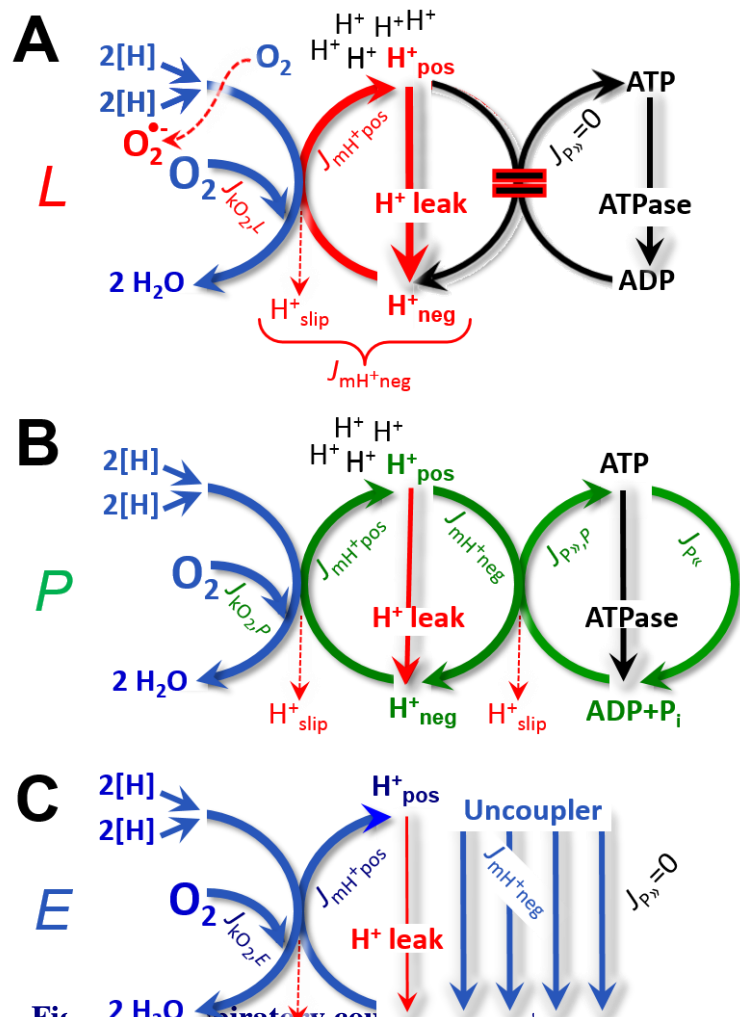



Figure 2 H₂O₂ respiratory coupling states and rates. (A) **LEAK-state and rate, L:** Phosphorylation is arrested, $J_{P>} = 0$, and catabolic O₂ flux, $J_{kO_2,L}$, is controlled mainly by the proton leak, $J_{mH^{+}neg,L}$, at maximum protonmotive force (**Figure 3**). (B) **OXPHOS-state and rate, P:** Phosphorylation, $J_{P>,P}$, is stimulated by kinetically-saturating [ADP] and [P_i], and is supported by a high protonmotive force. O₂ flux, $J_{kO_2,P}$, is well-coupled at a $P_{>}/O_2$ ratio of $J_{P>,P}/J_{kO_2,P}$. (C) **ET-state and rate, E:** Noncoupled respiration, $J_{kO_2,E}$, is maximum at optimum exogenous uncoupler concentration and phosphorylation is zero, $J_{P>} = 0$. See also **Figure 2**.

666 inhibition of the phosphorylation-pathway by inhibitors of F-ATPase—such as oligomycin, or
 667 of adenine nucleotide translocase—such as carboxyatractyloside. Adjustment of the nominal
 668 concentration of these inhibitors to the density of biological sample applied can minimize or
 669 avoid inhibitory side-effects exerted on ET-capacity or even some dyscoupling.

670 **Proton leak and uncoupled respiration:** Proton leak is a leak current of protons. The
 671 intrinsic proton leak is the *uncoupled* process in which protons diffuse across the mtIM in the
 672 dissipative direction of the downhill protonmotive force without coupling to phosphorylation
 673 (**Figure 5A**). The proton leak flux depends non-linearly on the protonmotive force (Garlid *et*
 674 *al.* 1989; Divakaruni and Brand 2011), it is a property of the mtIM and may be enhanced due
 675 to possible contaminations by free fatty acids. Inducible uncoupling mediated by uncoupling
 676 protein 1 (UCP1) is physiologically controlled, *e.g.*, in brown adipose tissue. UCP1 is a member
 677 of the mitochondrial carrier family which is involved in the translocation of protons across the
 678 mtIM (Klingenberg 2017). Consequently, the short-circuit diminishes the protonmotive force
 679 and stimulates electron transfer to O₂ and heat dissipation without phosphorylation of ADP.

680 **Cation cycling:** There can be other cation contributors to leak current including calcium
 681 and probably magnesium. Calcium current is balanced by mitochondrial Na⁺/Ca²⁺ exchange,
 682 which is balanced by Na⁺/H⁺ or K⁺/H⁺ exchanges. This is another effective uncoupling
 683 mechanism different from proton leak (**Table 2**).
 684
 685

Table 2. Terms on respiratory coupling and uncoupling.

Term	$J_{\text{K}O_2}$	$P \gg O_2$	Note		
acoupled		0	electron transfer in mitochondrial fragments without vectorial proton translocation (Figure 3)		
intrinsic, no protonophore added		uncoupled	L	0	non-phosphorylating LEAK-respiration (Figure 5A)
		proton leak-uncoupled		0	component of L , H ⁺ diffusion across the mtIM (Figure 3)
		decoupled		0	component of L , proton slip (Figure 3)
		loosely coupled		0	component of L , lower coupling due to superoxide formation and bypass of proton pumps (Figure 3)
		dyscoupled		0	pathologically, toxicologically, environmentally increased uncoupling, mitochondrial dysfunction
		inducibly uncoupled		0	by UCP1 or cation (<i>e.g.</i> , Ca ²⁺) cycling (Figure 3)
noncoupled	E	0	non-phosphorylating respiration stimulated to maximum flux at optimum exogenous uncoupler concentration (Figure 5C)		
well-coupled	P	high	phosphorylating respiration with an intrinsic LEAK component (Figure 5B)		
fully coupled	$P - L$	max.	OXPPOS-capacity corrected for LEAK-respiration (Figure 4)		

686
 687 **Proton slip and decoupled respiration:** Proton slip is the *decoupled* process in which
 688 protons are only partially translocated by a redox proton pump of the ET-pathways and slip
 689 back to the original vesicular compartment. The proton leak is the dominant contributor to the
 690 overall leak current in mammalian mitochondria incubated under physiological conditions at
 691 37 °C, whereas proton slip is increased at lower experimental temperature (Canton *et al.* 1995).

692 Proton slip can also happen in association with the F-ATPase, in which the proton slips downhill
 693 across the pump to the matrix without contributing to ATP synthesis. In each case, proton slip
 694 is a property of the proton pump and increases with the pump turnover rate.

695 **Electron leak and loosely coupled respiration:** Superoxide production by the ETS leads
 696 to a bypass of redox proton pumps and correspondingly lower P_{\gg}/O_2 ratio. This depends on the
 697 actual site of electron leak and the scavenging of hydrogen peroxide by cytochrome *c*, whereby
 698 electrons may re-enter the ETS with proton translocation by CIV.

699 **Loss of compartmental integrity and acoupled respiration:** Electron transfer and
 700 catabolic O_2 flux proceed without compartmental proton translocation in disrupted
 701 mitochondrial fragments. Such fragments form during mitochondrial isolation, and may not
 702 fully fuse to re-establish structurally intact mitochondria. Loss of mtIM integrity, therefore, is
 703 the cause of acoupled respiration, which is a nonvectorial dissipative process without control
 704 by the protonmotive force.

705 **Dyscoupled respiration:** Mitochondrial injuries may lead to *dyscoupling* as a
 706 pathological or toxicological cause of *uncoupled* respiration. Dyscoupling may involve any
 707 type of uncoupling mechanism, *e.g.*, opening the permeability transition pore. Dyscoupled
 708 respiration is distinguished from the experimentally induced *noncoupled* respiration in the ET-
 709 state (**Table 2**).

710 **OXPPOS-state (Figure 5B):** The OXPPOS-state is defined as the respiratory state with
 711 kinetically-saturating concentrations of O_2 , respiratory and phosphorylation substrates, and
 712 absence of exogenous uncoupler, which provides an estimate of the maximal respiratory
 713 capacity in the OXPPOS-state for any given ET-pathway state. Respiratory capacities at
 714 kinetically-saturating substrate concentrations provide reference values or upper limits of
 715 performance, aiming at the generation of data sets for comparative purposes. Physiological
 716 activities and effects of substrate kinetics can be evaluated relative to the OXPPOS-capacity.

717 As discussed previously, 0.2 mM ADP does not fully saturate flux in isolated
 718 mitochondria (Gnaiger 2001; Puchowicz *et al.* 2004); greater ADP concentration is required,
 719 particularly in permeabilized muscle fibres and cardiomyocytes, to overcome limitations by
 720 intracellular diffusion and by the reduced conductance of the mtOM (Jepihhina *et al.* 2011,
 721 Illaste *et al.* 2012, Simson *et al.* 2016), either through interaction with tubulin (Rostovtseva *et*
 722 *al.* 2008) or other intracellular structures (Birkedal *et al.* 2014). In permeabilized muscle fibre
 723 bundles of high respiratory capacity, the apparent K_m for ADP increases up to 0.5 mM (Saks *et*
 724 *al.* 1998), consistent with experimental evidence that >90% saturation is reached only at >5
 725 mM ADP (Pesta and Gnaiger 2012). Similar ADP concentrations are also required for accurate
 726 determination of OXPPOS-capacity in human clinical cancer samples and permeabilized cells
 727 (Klepinin *et al.* 2016; Koit *et al.* 2017). Whereas 2.5 to 5 mM ADP is sufficient to obtain the
 728 actual OXPPOS-capacity in many types of permeabilized tissue and cell preparations,
 729 experimental validation is required in each specific case.

730 **Electron transfer-state (Figure 5C):** The ET-state is defined as the *noncoupled* state
 731 with kinetically-saturating concentrations of O_2 , respiratory substrate and optimum *exogenous*
 732 uncoupler concentration for maximum O_2 flux. O_2 flux determined in the ET-state yields an
 733 estimate of ET-capacity. Inhibition of respiration is observed above optimum uncoupler
 734 concentrations. As a consequence of the nearly collapsed protonmotive force, the driving force
 735 is insufficient for phosphorylation, and $J_{P_{\gg}} = 0$.

736 **ROX state and Rox:** Besides the three fundamental coupling states of mitochondrial
 737 preparations, the state of residual O_2 consumption, ROX, is relevant to assess respiratory
 738 function. ROX is not a coupling state. The rate of residual oxygen consumption, *Rox*, is defined
 739 as O_2 consumption due to oxidative reactions measured after inhibition of ET—with rotenone,
 740 malonic acid and antimycin A. Cyanide and azide inhibit not only CIV but catalase and several
 741 peroxidases involved in *Rox*. However, high concentrations of antimycin A, but not rotenone
 742 or cyanide, inhibit peroxisomal acyl-CoA oxidase and D-amino acid oxidase (Vamecq *et al.*

1987). ROX represents a baseline that is used to correct respiration in defined coupling states. *Rox* is not necessarily equivalent to non-mitochondrial reduction of O₂, considering O₂-consuming reactions in mitochondria that are not related to ET—such as O₂ consumption in reactions catalyzed by monoamine oxidases (type A and B), monooxygenases (cytochrome P450 monooxygenases), dioxygenase (sulfur dioxygenase and trimethyllysine dioxygenase), and several hydroxylases. Even isolated mitochondrial fractions, especially those obtained from liver, may be contaminated by peroxisomes. This fact makes the exact determination of mitochondrial O₂ consumption and mitochondria-associated generation of reactive oxygen species complicated (Schönfeld *et al.* 2009; Speijer 2016; **Figure 1**). The dependence of ROX-linked O₂ consumption needs to be studied in detail together with non-ET enzyme activities, availability of specific substrates, O₂ concentration, and electron leakage leading to the formation of reactive oxygen species.

Quantitative relations: *E* may exceed or be equal to *P*. $E > P$ is observed in many types of mitochondria, varying between species, tissues and cell types (Gnaiger 2009). $E - P$ is the excess ET-capacity pushing the phosphorylation-flux (**Figure 2B**) to the limit of its *capacity of utilizing* the protonmotive force. In addition, the magnitude of $E - P$ depends on the tightness of respiratory coupling or degree of uncoupling, since an increase of *L* causes *P* to increase towards the limit of *E*. The *excess E-P* capacity, $E - P$, therefore, provides a sensitive diagnostic indicator of specific injuries of the phosphorylation-pathway, under conditions when *E* remains constant but *P* declines relative to controls (**Figure 4**). Substrate cocktails supporting simultaneous convergent electron transfer to the Q-junction for reconstitution of TCA cycle function establish pathway control states with high ET-capacity, and consequently increase the sensitivity of the $E - P$ assay.

E cannot theoretically be lower than *P*. $E < P$ must be discounted as an artefact, which may be caused experimentally by: (1) loss of oxidative capacity during the time course of the respirometric assay, since *E* is measured subsequently to *P*; (2) using insufficient uncoupler concentrations; (3) using high uncoupler concentrations which inhibit ET (Gnaiger 2008); (4) high oligomycin concentrations applied for measurement of *L* before titrations of uncoupler, when oligomycin exerts an inhibitory effect on *E*. On the other hand, the excess ET-capacity is overestimated if non-saturating [ADP] or [P_i] are used. See State 3 in the next section.

The net OXPHOS-capacity is calculated by subtracting *L* from *P* (**Figure 4**). Then the net $P \gg O_2$ equals $P \gg (P - L)$, wherein the dissipative LEAK component in the OXPHOS-state may be overestimated. This can be avoided by measuring LEAK-respiration in a state when the protonmotive force is adjusted to its slightly lower value in the OXPHOS-state—by titration of an ET inhibitor (Divakaruni and Brand 2011). Any turnover-dependent components of proton leak and slip, however, are underestimated under these conditions (Garlid *et al.* 1993). In general, it is inappropriate to use the term *ATP production* or *ATP turnover* for the difference of O₂ flux measured in states *P* and *L*. The difference $P - L$ is the upper limit of the part of OXPHOS-capacity that is freely available for ATP production (corrected for LEAK-respiration) and is fully coupled to phosphorylation with a maximum mechanistic stoichiometry (**Figure 4**).

784

785 2.3. Classical terminology for isolated mitochondria

786 ‘When a code is familiar enough, it ceases appearing like a code; one forgets that there
787 is a decoding mechanism. The message is identical with its meaning’ (Hofstadter 1979).
788

789 Chance and Williams (1955; 1956) introduced five classical states of mitochondrial
790 respiration and cytochrome redox states. **Table 3** shows a protocol with isolated mitochondria
791 in a closed respirometric chamber, defining a sequence of respiratory states. States and rates
792 are not specifically distinguished in this nomenclature.
793

794
795
796**Table 3. Metabolic states of mitochondria (Chance and Williams, 1956; Table V).**

State	[O ₂]	ADP level	Substrate level	Respiration rate	Rate-limiting substance
1	>0	Low	low	slow	ADP
2	>0	high	~0	slow	substrate
3	>0	high	high	fast	respiratory chain
4	>0	Low	high	slow	ADP
5	0	high	high	0	oxygen

797

798

799

800

State 1 is obtained after addition of isolated mitochondria to air-saturated isoosmotic/isotonic respiration medium containing P_i, but no fuel substrates and no adenylates, *i.e.*, AMP, ADP, ATP.

801

802

803

804

805

806

807

808

809

810

811

812

State 2 is induced by addition of a ‘high’ concentration of ADP (typically 100 to 300 μM), which stimulates respiration transiently on the basis of endogenous fuel substrates and phosphorylates only a small portion of the added ADP. State 2 is then obtained at a low respiratory activity limited by exhausted endogenous fuel substrate availability (**Table 3**). If addition of specific inhibitors of respiratory complexes—such as rotenone—does not cause a further decline of O₂ flux, State 2 is equivalent to the ROX state (See below.). If inhibition is observed, undefined endogenous fuel substrates are a confounding factor of pathway control, contributing to the effect of subsequently externally added substrates and inhibitors. In contrast to the original protocol, an alternative sequence of titration steps is frequently applied, in which the alternative ‘State 2’ has an entirely different meaning, when this second state is induced by addition of fuel substrate without ADP (LEAK-state; in contrast to State 2 defined in **Table 1** as a ROX state), followed by addition of ADP.

813

814

815

816

817

818

819

820

821

822

823

824

825

State 3 is the state stimulated by addition of fuel substrates while the ADP concentration is still high (**Table 3**) and supports coupled energy transformation through oxidative phosphorylation. ‘High ADP’ is a concentration of ADP specifically selected to allow the measurement of State 3 to State 4 transitions of isolated mitochondria in a closed respirometric chamber. Repeated ADP titration re-establishes State 3 at ‘high ADP’. Starting at O₂ concentrations near air-saturation (ca. 200 μM O₂ at sea level and 37 °C), the total ADP concentration added must be low enough (typically 100 to 300 μM) to allow phosphorylation to ATP at a coupled O₂ flux that does not lead to O₂ depletion during the transition to State 4. In contrast, kinetically-saturating ADP concentrations usually are 10-fold higher than ‘high ADP’, *e.g.*, 2.5 mM in isolated mitochondria. The abbreviation State 3u is occasionally used in bioenergetics, to indicate the state of respiration after titration of an uncoupler, without sufficient emphasis on the fundamental difference between OXPHOS-capacity (*well-coupled* with an *endogenous* uncoupled component) and ET-capacity (*noncoupled*).

826

827

828

829

830

831

832

833

834

835

836

837

State 4 is a LEAK-state that is obtained only if the mitochondrial preparation is intact and well-coupled. Depletion of ADP by phosphorylation to ATP causes a decline of O₂ flux in the transition from State 3 to State 4. Under the conditions of State 4, a maximum protonmotive force and high ATP/ADP ratio are maintained. The gradual decline of Y_{P_»/O₂} towards diminishing [ADP] at State 4 must be taken into account for calculation of P_»/O₂ ratios (Gnaiger 2001). State 4 respiration, L_T (**Table 1**), reflects intrinsic proton leak and ATP hydrolysis activity. O₂ flux in State 4 is an overestimation of LEAK-respiration if the contaminating ATP hydrolysis activity recycles some ATP to ADP, J_{P_«}, which stimulates respiration coupled to phosphorylation, J_{P_»} > 0. This can be tested by inhibition of the phosphorylation-pathway using oligomycin, ensuring that J_{P_»} = 0 (State 4o). Alternatively, sequential ADP titrations re-establish State 3, followed by State 3 to State 4 transitions while sufficient O₂ is available. Anoxia may be reached, however, before exhaustion of ADP (State 5).

838 **State 5** is the state after exhaustion of O₂ in a closed respirometric chamber. Diffusion of
 839 O₂ from the surroundings into the aqueous solution may be a confounding factor preventing
 840 complete anoxia (Gnaiger 2001). Chance and Williams (1955) provide an alternative definition
 841 of State 5, which gives it the different meaning of ROX versus anoxia: ‘State 5 may be obtained
 842 by antimycin A treatment or by anaerobiosis’.

843 In **Table 3**, only States 3 and 4 (and ‘State 2’ in the alternative protocol: addition of fuel
 844 substrates without ADP; not included in the table) are coupling control states, with the
 845 restriction that O₂ flux in State 3 may be limited kinetically by non-saturating ADP
 846 concentrations (**Table 1**).

847
848

849 3. Normalization: fluxes and flows

850

851 3.1. Normalization: system or sample

852

853 The term *rate* is not sufficiently defined to be useful for reporting data (**Figure 6**). The
 854 inconsistency of the meanings of rate becomes fully apparent when considering Galileo
 855 Galilei’s famous principle, that ‘bodies of different weight all fall at the same rate (have a
 856 constant acceleration)’ (Coopersmith 2010).

857

858 **Figure 6. Flow and flux, with system- or sample-specific normalization**

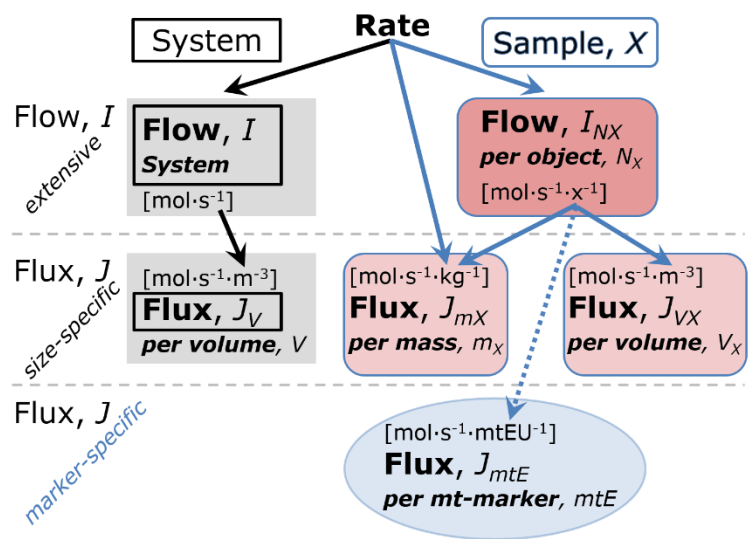
859 Different meanings of rate may lead to confusion, if the normalization is not sufficiently
 860 specified. Results are frequently expressed as mass-specific *flux*, J_{mX} , per mg protein, dry or wet
 861 weight (mass). Cell volume, V_{cell} , may be used for normalization (volume-specific flux, $J_{V\text{cell}}$),
 862 which must be clearly distinguished from flow per cell, $I_{N\text{cell}}$, or flux, J_V , expressed for
 863 methodological reasons per volume of the measurement system. For details see **Table 4**.

864

865 **Flow per system, I :** In a generalization of electrical terms, flow as an extensive quantity
 866 (I ; per system) is distinguished from flux as a size-specific quantity (J ; per system size) (**Figure**
 867 **6**). Electric current is flow, I_{el} [$\text{A} \equiv \text{C} \cdot \text{s}^{-1}$] per system (extensive quantity). When dividing this
 868 extensive quantity by system size (cross-sectional area of a ‘wire’), a size-specific quantity is
 869 obtained, which is flux (current density), J_{el} [$\text{A} \cdot \text{m}^{-2} = \text{C} \cdot \text{s}^{-1} \cdot \text{m}^{-2}$].

870 **Extensive quantities:** An extensive quantity increases proportionally with system size.
 871 The magnitude of an extensive quantity is completely additive for non-interacting
 872 subsystems—such as mass or flow expressed per defined system. The magnitude of these
 873 quantities depends on the extent or size of the system (Cohen *et al.* 2008).

874 **Size-specific quantities:** ‘The adjective *specific* before the name of an extensive quantity
 875 is often used to mean *divided by mass*’ (Cohen *et al.* 2008). In this system-paradigm, mass-
 876 specific flux is flow divided by mass of the *system* (the total mass of everything within the
 877 measuring chamber or reactor). A mass-specific quantity is independent of the extent of non-
 878 interacting homogenous subsystems. Tissue-specific quantities (related to the *sample* in
 879 contrast to the *system*) are of fundamental interest in the field of comparative mitochondrial



890 physiology, where *specific* refers to the *type of the sample* rather than *mass of the system*. The
 891 term *specific*, therefore, must be clarified; *sample-specific*, e.g., muscle mass-specific
 892 normalization, is distinguished from *system-specific* quantities (mass or volume; **Figure 6**).
 893

894 **Box 2: Metabolic fluxes and flows: vectorial and scalar**

895
 896 Fluxes are *vectors*, if they have *spatial* geometric direction in addition to magnitude.
 897 Electric charge per unit time is electric flow or current, $I_{el} = dQ_{el} \cdot dt^{-1}$ [A]. When expressed per
 898 unit cross-sectional area, A [m^2], a vector flux is obtained, which is current density (surface-
 899 density of flow) perpendicular to the direction of flux, $J_{el} = I_{el} \cdot A^{-1}$ [$A \cdot m^{-2}$] (Cohen et al. 2008).
 900 For all transformations *flows*, I_{tr} , are defined as extensive quantities. Vector and scalar *fluxes*
 901 are obtained as $J_{tr} = I_{tr} \cdot A^{-1}$ [$mol \cdot s^{-1} \cdot m^{-2}$] and $J_{tr} = I_{tr} \cdot V^{-1}$ [$mol \cdot s^{-1} \cdot m^{-3}$], expressing flux as an area-
 902 specific vector or volume-specific vectorial or scalar quantity, respectively (Gnaiger 1993b).

903 We suggest to define: (1) *vectorial* fluxes, which are translocations as functions of
 904 *gradients* with direction in geometric space in continuous systems; (2) *vectorial* fluxes, which
 905 describe translocations in discontinuous systems and are restricted to information on
 906 *compartmental differences* (**Figure 2C**, transmembrane proton flux); and (3) *scalar* fluxes,
 907 which are transformations in a *homogenous* system (**Figure 2C**, catabolic O_2 flux, J_{kO_2}).

908 Vectorial transmembrane proton fluxes, J_{mH^+pos} and J_{mH^+neg} , are analyzed in a
 909 heterogenous compartmental system as a quantity with *directional* but not *spatial* information.
 910 Translocation of protons across the mtIM has a defined direction, either from the negative
 911 compartment (matrix space; negative, neg-compartment) to the positive compartment (inter-
 912 membrane space; positive, pos-compartment) or *vice versa* (**Figure 2C**). The arrows defining
 913 the direction of the translocation between the two vesicular compartments may point upwards
 914 or downwards, right or left, without any implication that these are actual directions in space.
 915 The pos-compartment is neither above nor below the neg-compartment in a spatial sense, but
 916 can be visualized arbitrarily in a figure in the upper position (**Figure 2C**). In general, the
 917 *compartmental direction* of vectorial translocation from the neg-compartment to the pos-
 918 compartment is defined by assigning the initial and final state as *ergodynamic compartments*,
 919 $H^+_{neg} \rightarrow H^+_{pos}$ or $0 = -1 H^+_{neg} + 1 H^+_{pos}$, related to work (erg = work) that must be performed to
 920 lift the proton from a lower to a higher electrochemical potential or from the lower to the higher
 921 ergodynamic compartment (Gnaiger 1993b).

922 In analogy to *vectorial* translocation, the direction of a *scalar* chemical reaction, $A \rightarrow B$
 923 or $0 = -1 A + 1 B$, is defined by assigning substrates and products, A and B, as ergodynamic
 924 compartments. O_2 is defined as a substrate in respiratory O_2 consumption, which together with
 925 the fuel substrates comprises the substrate compartment of the catabolic reaction. Volume-
 926 specific scalar O_2 flux is coupled to vectorial translocation, yielding the H^+_{pos}/O_2 ratio (**Figure**
 927 **2**).

928 3.2. Normalization for system-size: flux per chamber volume

931 **System-specific flux, J_{V,O_2} :** The experimental system (experimental chamber) is part of
 932 the measurement apparatus, separated from the environment as an isolated, closed, open,
 933 isothermal or non-isothermal system (**Table 4**). On another level, we distinguish between (1)
 934 the *system* with volume V and mass m defined by the system boundaries, and (2) the *sample* or
 935 *objects* with volume V_X and mass m_X which are enclosed in the experimental chamber (**Figure**
 936 **6**). Metabolic O_2 flow per object, $I_{O_2/X}$, increases as the mass of the object is increased. Sample
 937 mass-specific O_2 flux, $J_{O_2/mX}$ should be independent of the mass of the sample studied in the
 938 instrument chamber, but system volume-specific O_2 flux, J_{V,O_2} (per volume of the instrument
 939 chamber), should increase in direct proportion to the mass of the sample in the chamber.
 940 Whereas J_{V,O_2} depends on mass-concentration of the sample in the chamber, it should be

941 independent of the chamber (system) volume at constant sample mass. There are practical
 942 limitations to increase the mass-concentration of the sample in the chamber, when one is
 943 concerned about crowding effects and instrumental time resolution.

944 When the reactor volume does not change during the reaction, which is typical for liquid
 945 phase reactions, the volume-specific *flux of a chemical reaction* r is the time derivative of the
 946 advancement of the reaction per unit volume, $J_{V,rB} = d_r\zeta_B/dt \cdot V^{-1}$ [(mol·s⁻¹)·L⁻¹]. The *rate of*
 947 *concentration change* is dc_B/dt [(mol·L⁻¹)·s⁻¹], where concentration is $c_B = n_B/V$. There is a
 948 difference between (1) J_{V,rO_2} [mol·s⁻¹·L⁻¹] and (2) rate of concentration change [mol·L⁻¹·s⁻¹].
 949 These merge to a single expression only in closed systems. In open systems, external fluxes
 950 (such as O₂ supply) are distinguished from internal transformations (catabolic flux, O₂
 951 consumption). In a closed system, external flows of all substances are zero and O₂ consumption
 952 (internal flow of catabolic reactions k), I_{kO_2} [pmol·s⁻¹], causes a decline of the amount of O₂ in
 953 the system, n_{O_2} [nmol]. Normalization of these quantities for the volume of the system, V [L ≡
 954 dm³], yields volume-specific O₂ flux, $J_{V,kO_2} = I_{kO_2}/V$ [nmol·s⁻¹·L⁻¹], and O₂ concentration, [O₂]
 955 or $c_{O_2} = n_{O_2}/V$ [μmol·L⁻¹ = μM = nmol·mL⁻¹]. Instrumental background O₂ flux is due to external
 956 flux into a non-ideal closed respirometer; then total volume-specific flux has to be corrected for
 957 instrumental background O₂ flux—O₂ diffusion into or out of the instrumental chamber. J_{V,kO_2}
 958 is relevant mainly for methodological reasons and should be compared with the accuracy of
 959 instrumental resolution of background-corrected flux, *e.g.*, ±1 nmol·s⁻¹·L⁻¹ (Gnaiger 2001).
 960 ‘Metabolic’ or catabolic indicates O₂ flux, J_{kO_2} , corrected for: (1) instrumental background O₂
 961 flux; (2) chemical background O₂ flux due to autoxidation of chemical components added to
 962 the incubation medium; and (3) *Rox* for O₂-consuming side reactions unrelated to the catabolic
 963 pathway k .

964 3.3. Normalization: per sample

965 The challenges of measuring mitochondrial respiratory flux are matched by those of
 966 normalization. Application of common and defined units is required for direct transfer of
 967 reported results into a database. The second [s] is the *SI* unit for the base quantity *time*. It is also
 968 the standard time-unit used in solution chemical kinetics. A rate may be considered as the
 969 numerator and normalization as the complementary denominator, which are tightly linked in
 970 reporting the measurements in a format commensurate with the requirements of a database.
 971 Normalization (**Table 4**) is guided by physicochemical principles, methodological
 972 considerations, and conceptual strategies (**Figure 7**).

973 **Sample concentration, C_{mX} :** Normalization for sample concentration is required to
 974 report respiratory data. Considering a tissue or cells as the sample, X , the sample mass is m_X
 975 [mg], which is frequently measured as wet or dry weight, W_w or W_d [mg], respectively, or as
 976 amount of tissue or cell protein, m_{protein} . In the case of permeabilized tissues, cells, and
 977 homogenates, the sample concentration, $C_{mX} = m_X/V$ [g·L⁻¹ = mg·mL⁻¹], is the mass of the
 978 subsample of tissue that is transferred into the instrument chamber.

979 **Mass-specific flux, $J_{O_2/mX}$:** Mass-specific flux is obtained by expressing respiration per
 980 mass of sample, m_X [mg]. X is the type of sample—isolated mitochondria, tissue homogenate,
 981 permeabilized fibres or cells. Volume-specific flux is divided by mass concentration of X , $J_{O_2/mX}$
 982 = $J_{V,O_2}/C_{mX}$; or flow per cell is divided by mass per cell, $J_{O_2/mcell} = I_{O_2/cell}/M_{cell}$. If mass-specific
 983 O₂ flux is constant and independent of sample size (expressed as mass), then there is no
 984 interaction between the subsystems. A 1.5 mg and a 3.0 mg muscle sample respire at identical
 985 mass-specific flux. Mass-specific O₂ flux, however, may change with the mass of a tissue
 986 sample, cells or isolated mitochondria in the measuring chamber, in which the nature of the
 987 interaction becomes an issue. Therefore, cell density must be optimized, particularly in
 988 experiments carried out in wells, considering the confluency of the cell monolayer or clumps
 989 of cells (Salabei *et al.* 2014).
 990
 991

Table 4. Sample concentrations and normalization of flux.

Expression	Symbol	Definition	Unit	Notes
Sample				
identity of sample	X	object: cell, tissue, animal, patient		
number of sample entities X	N_X	number of objects	x	
mass of sample X	m_X		kg	1
mass of object X	M_X	$M_X = m_X \cdot N_X^{-1}$	$\text{kg} \cdot \text{x}^{-1}$	1
Mitochondria				
mitochondria	mt	$X = \text{mt}$		
amount of mt-elements	mtE	quantity of mt-marker	mtEU	
Concentrations				
object number concentration	C_{NX}	$C_{NX} = N_X \cdot V^{-1}$	$\text{x} \cdot \text{m}^{-3}$	2
sample mass concentration	C_{mX}	$C_{mX} = m_X \cdot V^{-1}$	$\text{kg} \cdot \text{m}^{-3}$	
mitochondrial concentration	C_{mtE}	$C_{mtE} = mtE \cdot V^{-1}$	$\text{mtEU} \cdot \text{m}^{-3}$	3
specific mitochondrial density	D_{mtE}	$D_{mtE} = mtE \cdot m_X^{-1}$	$\text{mtEU} \cdot \text{kg}^{-1}$	4
mitochondrial content, mtE per object X	mtE_X	$mtE_X = mtE \cdot N_X^{-1}$	$\text{mtEU} \cdot \text{x}^{-1}$	5
O₂ flow and flux				
flow, system	I_{O_2}	internal flow	$\text{mol} \cdot \text{s}^{-1}$	6
volume-specific flux	J_{V,O_2}	$J_{V,O_2} = I_{O_2} \cdot V^{-1}$	$\text{mol} \cdot \text{s}^{-1} \cdot \text{m}^{-3}$	7
flow per object X	$I_{O_2/X}$	$I_{O_2/X} = J_{V,O_2} \cdot C_{NX}^{-1}$	$\text{mol} \cdot \text{s}^{-1} \cdot \text{x}^{-1}$	8
mass-specific flux	$J_{O_2/mX}$	$J_{O_2/mX} = J_{V,O_2} \cdot C_{mX}^{-1}$	$\text{mol} \cdot \text{s}^{-1} \cdot \text{kg}^{-1}$	9
mitochondria-specific flux	$J_{O_2/mtE}$	$J_{O_2/mtE} = J_{V,O_2} \cdot C_{mtE}^{-1}$	$\text{mol} \cdot \text{s}^{-1} \cdot \text{mtEU}^{-1}$	10

- 994 1 The SI prefix k is used for the SI base unit of mass (kg = 1,000 g). In praxis, various SI prefixes are
995 used for convenience, to make numbers easily readable, e.g., 1 mg tissue, cell or mitochondrial mass
996 instead of 0.000001 kg.
- 997 2 In case sample $X = \text{cells}$, the object number concentration is $C_{N_{\text{cell}}} = N_{\text{cell}} \cdot V^{-1}$, and volume may be
998 expressed in [$\text{dm}^3 \equiv \text{L}$] or [$\text{cm}^3 = \text{mL}$]. See **Table 5** for different object types.
- 999 3 mt-concentration is an experimental variable, dependent on sample concentration: (1) $C_{mtE} = mtE \cdot V^{-1}$;
1000 (2) $C_{mtE} = mtE_X \cdot C_{NX}$; (3) $C_{mtE} = C_{mX} \cdot D_{mtE}$.
- 1001 4 If the amount of mitochondria, mtE , is expressed as mitochondrial mass, then D_{mtE} is the mass
1002 fraction of mitochondria in the sample. If mtE is expressed as mitochondrial volume, V_{mt} , and the
1003 mass of sample, m_X , is replaced by volume of sample, V_X , then D_{mtE} is the volume fraction of
1004 mitochondria in the sample.
- 1005 5 $mtE_X = mtE \cdot N_X^{-1} = C_{mtE} \cdot C_{NX}^{-1}$.
- 1006 6 O₂ can be replaced by other chemicals B to study different reactions, e.g., ATP, H₂O₂, or vesicular
1007 compartmental translocations, e.g., Ca²⁺.
- 1008 7 I_{O_2} and V are defined per instrument chamber as a system of constant volume (and constant
1009 temperature), which may be closed or open. I_{O_2} is abbreviated for I_{r,O_2} , i.e., the metabolic or internal
1010 O₂ flow of the chemical reaction r in which O₂ is consumed, hence the negative stoichiometric
1011 number, $\nu_{O_2} = -1$. $I_{r,O_2} = d_r n_{O_2} / dt \cdot \nu_{O_2}^{-1}$. If r includes all chemical reactions in which O₂ participates, then
1012 $d_r n_{O_2} = dn_{O_2} - d_e n_{O_2}$, where dn_{O_2} is the change in the amount of O₂ in the instrument chamber and $d_e n_{O_2}$
1013 is the amount of O₂ added externally to the system. At steady state, by definition $dn_{O_2} = 0$, hence $d_r n_{O_2}$
1014 $= -d_e n_{O_2}$.
- 1015 8 J_{V,O_2} is an experimental variable, expressed per volume of the instrument chamber.
- 1016 9 $I_{O_2/X}$ is a physiological variable, depending on the size of entity X .
- 1017 10 There are many ways to normalize for a mitochondrial marker, that are used in different experimental
1018 approaches: (1) $J_{O_2/mtE} = J_{V,O_2} \cdot C_{mtE}^{-1}$; (2) $J_{O_2/mtE} = J_{V,O_2} \cdot C_{mX}^{-1} \cdot D_{mtE}^{-1} = J_{O_2/mX} \cdot D_{mtE}^{-1}$; (3) $J_{O_2/mtE} =$
1019 $J_{V,O_2} \cdot C_{NX}^{-1} \cdot mtE_X^{-1} = I_{O_2/X} \cdot mtE_X^{-1}$; (4) $J_{O_2/mtE} = I_{O_2} \cdot mtE^{-1}$. The mt-elemental unit [mtEU] varies between
1020 different mt-markers.

1021

Table 5. Sample types, X, abbreviations, and quantification.

Identity of sample	X	N_X	Mass ^a	Volume	mt-Marker
mitochondrial preparation	mt-prep	[x]	[kg]	[m ³]	[mtEU]
isolated mitochondria	imt		m_{mt}	V_{mt}	mtE
tissue homogenate	thom		m_{thom}		mtE_{thom}
permeabilized tissue	pti		m_{pti}		mtE_{pti}
permeabilized fibre	pfi		m_{pfi}		mtE_{pfi}
permeabilized cell	pce	N_{pce}	M_{pce}	V_{pce}	mtE_{pce}
cells ^b	cell	N_{cell}	M_{cell}	V_{cell}	mtE_{cell}
intact cell, viable cell	vce	N_{vce}	M_{vce}	V_{vce}	
dead cell	dce	N_{dce}	M_{dce}	V_{dce}	
organism	org	N_{org}	M_{org}	V_{org}	

1022

^a Instead of mass, the wet weight or dry weight is frequently stated, W_w or W_d .

1023

m_X is mass of the sample [kg], M_X is mass of the object [kg·x⁻¹].

1024

^b Total cell count, $N_{cell} = N_{vce} + N_{dce}$

1025

1026

Number concentration, C_{NX} : C_{NX} is the experimental *number concentration* of sample X. In the case of cells or animals, e.g., nematodes, $C_{NX} = N_X/V$ [x·L⁻¹], where N_X is the number of cells or organisms in the chamber (**Table 4**).

1027

1028

1029

Flow per object, $I_{O_2/X}$: A special case of normalization is encountered in respiratory studies with permeabilized (or intact) cells. If respiration is expressed per cell, the O₂ flow per measurement system is replaced by the O₂ flow per cell, $I_{O_2/cell}$ (**Table 4**). O₂ flow can be calculated from volume-specific O₂ flux, J_{V,O_2} [nmol·s⁻¹·L⁻¹] (per V of the measurement chamber [L]), divided by the number concentration of cells, $C_{Ncell} = N_{cell}/V$ [cell·L⁻¹], where N_{cell} is the number of cells in the chamber. The total cell count is the sum of viable and dead cells, $N_{cell} = N_{vce} + N_{dce}$ (**Table 5**). The cell viability index, $CVI = N_{vce}/N_{cell}$, is the ratio of viable cells (N_{vce} ; before experimental permeabilization) per total cell count. After experimental permeabilization, all cells are permeabilized, $N_{pce} = N_{cell}$. The cell viability index can be used to normalize respiration for the number of cells that have been viable before experimental permeabilization, $I_{O_2/vce} = I_{O_2/cell}/CVI$, considering that mitochondrial respiratory dysfunction in dead cells should be eliminated as a confounding factor.

1030

1031

1032

1033

1034

1035

1036

1037

1038

1039

1040

Cellular O₂ flow can be compared between cells of identical size. To take into account changes and differences in cell size, normalization is required to obtain cell size-specific or mitochondrial marker-specific O₂ flux (Renner *et al.* 2003).

1041

1042

1043

1044

1045

1046

1047

1048

1049

1050

1051

1052

The complexity changes when the sample is a whole organism studied as an experimental model. The scaling law in respiratory physiology reveals a strong interaction of O₂ flow and individual body mass of an organism, since *basal* metabolic rate (flow) does not increase linearly with body mass, whereas *maximum* mass-specific O₂ flux, \dot{V}_{O_2max} or \dot{V}_{O_2peak} , is approximately constant across a large range of individual body mass (Weibel and Hoppeler 2005), with individuals, breeds, and species deviating substantially from this relationship. \dot{V}_{O_2peak} of human endurance athletes is 60 to 80 mL O₂·min⁻¹·kg⁻¹ body mass, converted to $J_{O_2peak/M}$ of 45 to 60 nmol·s⁻¹·g⁻¹ (Gnaiger 2014; **Table 6**).

1051

1052

1053

1054

3.4. Normalization for mitochondrial content

1055

1056

1057

1058

1059

1060

Tissues can contain multiple cell populations that may have distinct mitochondrial subtypes. Mitochondria undergo dynamic fission and fusion cycles, and can exist in multiple stages and sizes that may be altered by a range of factors. The isolation of mitochondria (often achieved through differential centrifugation) can therefore yield a subsample of the mitochondrial types present in a tissue, depending on the isolation protocols utilized (e.g., centrifugation speed). This possible bias should be taken into account when planning

1061 experiments using isolated mitochondria. Different sizes of mitochondria are enriched at
 1062 specific centrifugation speeds, which can be used strategically for isolation of mitochondrial
 1063 subpopulations.

1064 Part of the mitochondrial content of a tissue is lost during preparation of isolated
 1065 mitochondria. The fraction of isolated mitochondria obtained from a tissue sample is expressed
 1066 as mitochondrial recovery. At a high mitochondrial recovery the fraction of isolated
 1067 mitochondria is more representative of the total mitochondrial population than in preparations
 1068 characterized by low recovery. Determination of the mitochondrial recovery and yield is based
 1069 on measurement of the concentration of a mitochondrial marker in the stock of isolated
 1070 mitochondria, $C_{mtE,stock}$, and crude tissue homogenate, $C_{mtE,thom}$, which simultaneously provides
 1071 information on the specific mitochondrial density in the sample, D_{mtE} (**Table 4**).

1072 Normalization is a problematic subject; it is essential to consider the question of the study.
 1073 If the study aims at comparing tissue performance—such as the effects of a treatment on a
 1074 specific tissue, then normalization for tissue mass or protein content is appropriate. However,
 1075 if the aim is to find differences on mitochondrial function independent of mitochondrial density
 1076 (**Table 4**), then normalization to a mitochondrial marker is imperative (**Figure 7**). One cannot
 1077 assume that quantitative changes in various markers—such as mitochondrial proteins—
 1078 necessarily occur in parallel with one another. It should be established that the marker chosen
 1079 is not selectively altered by the performed treatment. In conclusion, the normalization must
 1080 reflect the question under investigation to reach a satisfying answer. On the other hand, the goal
 1081 of comparing results across projects and institutions requires standardization on normalization
 1082 for entry into a databank.

1083

Flow, Performance	=	Element function	x	Element density	x	Size of object
$\frac{\text{mol}\cdot\text{s}^{-1}}{\text{x}}$	=	$\frac{\text{mol}\cdot\text{s}^{-1}}{x_{mtE}}$	·	$\frac{x_{mtE}}{\text{kg}}$	·	$\frac{\text{kg}}{\text{x}}$

A	Flow	=	mt-specific flux	x	mt-structure, functional elements
	$I_{O_2/X}$	=	$J_{O_2/mtE}$	·	mtE_X
					$\frac{mtE_X}{M_X} \cdot M_X$

$I_{O_2/X}$	=	$J_{O_2/mtE}$	·	D_{mtE}	·	M_X
-------------	---	---------------	---	-----------	---	-------

$\frac{I_{O_2/X}}{M_X}$	=	$\frac{I_{O_2/X}}{mtE_X}$	·	$\frac{mtE_X}{M_X}$
-------------------------	---	---------------------------	---	---------------------

B	$I_{O_2/X}$	=	$J_{O_2/MX}$	·	M_X
	Flow	=	Object mass- specific flux	x	Mass of object

1084

1085 **Figure 7. Structure-function analysis of performance of an organism, organ or tissue, or**
 1086 **a cell (sample entity, X)**

1087 O_2 flow, $I_{O_2/X}$, is the product of performance per functional element (element function,
 1088 mitochondria-specific flux), element density (mitochondrial density, D_{mtE}), and size of entity X
 1089 (mass, M_X). (**A**) Structured analysis: performance is the product of mitochondrial *function* (mt-
 1090 specific flux) and *structure* (functional elements; D_{mtE} times mass of X). (**B**) Unstructured
 1091 analysis: performance is the product of *entity mass-specific flux*, $J_{O_2/MX} = I_{O_2/X}/M_X = I_{O_2}/m_X$
 1092 [$\text{mol}\cdot\text{s}^{-1}\cdot\text{kg}^{-1}$] and *size of entity*, expressed as mass of X ; $M_X = m_X \cdot N_X^{-1}$ [$\text{kg}\cdot\text{x}^{-1}$]. See **Table 4** for
 1093 further explanation of quantities and units. Modified from Gnaiger (2014).

1094 **Mitochondrial concentration, C_{mtE} , and mitochondrial markers:** Mitochondrial
 1095 organelles comprise a dynamic cellular reticulum in various states of fusion and fission. Hence,
 1096 the definition of an "amount" of mitochondria is often misconceived: mitochondria cannot be
 1097 counted reliably as a number of occurring elements. Therefore, quantification of the "amount"
 1098 of mitochondria depends on the measurement of chosen mitochondrial markers. 'Mitochondria
 1099 are the structural and functional elemental units of cell respiration' (Gnaiger 2014). The
 1100 quantity of a mitochondrial marker can reflect the amount of *mitochondrial elements*, mtE ,
 1101 expressed in various mitochondrial elemental units [mtEU] specific for each measured mt-
 1102 marker (**Table 4**). However, since mitochondrial quality may change in response to stimuli—
 1103 particularly in mitochondrial dysfunction and after exercise training (Pesta *et al.* 2011; Campos
 1104 *et al.* 2017)—some markers can vary while others are unchanged: (1) Mitochondrial volume
 1105 and membrane area are structural markers, whereas mitochondrial protein mass is frequently
 1106 used as a marker for isolated mitochondria. (2) Molecular and enzymatic mitochondrial markers
 1107 (amounts or activities) can be selected as matrix markers, *e.g.*, citrate synthase activity, mtDNA;
 1108 mtIM-markers, *e.g.*, cytochrome *c* oxidase activity, *aa*₃ content, cardiolipin, or mtOM-markers,
 1109 *e.g.*, TOM20. (3) Extending the measurement of mitochondrial marker enzyme activity to
 1110 mitochondrial pathway capacity, ET- or OXPHOS-capacity can be considered as an integrative
 1111 functional mitochondrial marker.

1112 Depending on the type of mitochondrial marker, the mitochondrial elements, mtE , are
 1113 expressed in marker-specific units. Mitochondrial concentration in the measurement chamber
 1114 and the tissue of origin are quantified as (1) a quantity for normalization in functional analyses,
 1115 C_{mtE} , and (2) a physiological output that is the result of mitochondrial biogenesis and
 1116 degradation, D_{mtE} , respectively (**Table 4**). It is recommended, therefore, to distinguish
 1117 *experimental mitochondrial concentration*, $C_{mtE} = mtE/V$ and *physiological mitochondrial*
 1118 *density*, $D_{mtE} = mtE/m_X$. Then mitochondrial density is the amount of mitochondrial elements
 1119 per mass of tissue, which is a biological variable (**Figure 7**). The experimental variable is
 1120 mitochondrial density multiplied by sample mass concentration in the measuring chamber, C_{mtE}
 1121 $= D_{mtE} \cdot C_{mX}$, or mitochondrial content multiplied by sample number concentration, $C_{mtE} =$
 1122 $mtE_X \cdot C_{NX}$ (**Table 4**).

1123 **Mitochondria-specific flux, $J_{O_2/mtE}$:** Volume-specific metabolic O_2 flux depends on: (1)
 1124 the sample concentration in the volume of the instrument chamber, C_{mX} , or C_{NX} ; (2) the
 1125 mitochondrial density in the sample, $D_{mtE} = mtE/m_X$ or $mtE_X = mtE/N_X$; and (3) the specific
 1126 mitochondrial activity or performance per elemental mitochondrial unit, $J_{O_2/mtE} = J_{V,O_2}/C_{mtE}$
 1127 [$\text{mol}\cdot\text{s}^{-1}\cdot\text{mtEU}^{-1}$] (**Table 4**). Obviously, the numerical results for $J_{O_2/mtE}$ vary with the type of
 1128 mitochondrial marker chosen for measurement of mtE and $C_{mtE} = mtE/V$ [$\text{mtEU}\cdot\text{m}^{-3}$].

1129 3.5. Evaluation of mitochondrial markers

1130 Different methods are implicated in the quantification of mitochondrial markers and have
 1131 different strengths. Some problems are common for all mitochondrial markers, mtE : (1)
 1132 Accuracy of measurement is crucial, since even a highly accurate and reproducible
 1133 measurement of O_2 flux results in an inaccurate and noisy expression if normalized by a biased
 1134 and noisy measurement of a mitochondrial marker. This problem is acute in mitochondrial
 1135 respiration because the denominators used (the mitochondrial markers) are often small moieties
 1136 of which accurate and precise determination is difficult. This problem can be avoided when O_2
 1137 fluxes measured in substrate-uncoupler-inhibitor titration protocols are normalized for flux in
 1138 a defined respiratory reference state, which is used as an *internal* marker and yields flux control
 1139 ratios, *FCRs*. *FCRs* are independent of *externally* measured markers and, therefore, are
 1140 statistically robust, considering the limitations of ratios in general (Jasienski and Bazzaz 1999).
 1141 *FCRs* indicate qualitative changes of mitochondrial respiratory control, with highest
 1142 quantitative resolution, separating the effect of mitochondrial density or concentration on $J_{O_2/mX}$
 1143

1145 and $I_{O_2/X}$ from that of function per elemental mitochondrial marker, $J_{O_2/mtE}$ (Pesta *et al.* 2011;
 1146 Gnaiger 2014). (2) If mitochondrial quality does not change and only the amount of
 1147 mitochondria varies as a determinant of mass-specific flux, any marker is equally qualified in
 1148 principle; then in practice selection of the optimum marker depends only on the accuracy and
 1149 precision of measurement of the mitochondrial marker. (3) If mitochondrial flux control ratios
 1150 change, then there may not be any best mitochondrial marker. In general, measurement of
 1151 multiple mitochondrial markers enables a comparison and evaluation of normalization for a
 1152 variety of mitochondrial markers. Particularly during postnatal development, the activity of
 1153 marker enzymes—such as cytochrome *c* oxidase and citrate synthase—follows different time
 1154 courses (Drahota *et al.* 2004). Evaluation of mitochondrial markers in healthy controls is
 1155 insufficient for providing guidelines for application in the diagnosis of pathological states and
 1156 specific treatments.

1157 In line with the concept of the respiratory control ratio (Chance and Williams 1955a), the
 1158 most readily used normalization is that of flux control ratios and flux control factors (Gnaiger
 1159 2014). Selection of the state of maximum flux in a protocol as the reference state has the
 1160 advantages of: (1) internal normalization; (2) statistical linearization of the response in the range
 1161 of 0 to 1; and (3) consideration of maximum flux for integrating a large number of elemental
 1162 steps in the OXPHOS- or ET-pathways. This reduces the risk of selecting a functional marker
 1163 that is specifically altered by the treatment or pathology, yet increases the chance that the highly
 1164 integrative pathway is disproportionately affected, *e.g.*, the OXPHOS- rather than ET-pathway
 1165 in case of an enzymatic defect in the phosphorylation-pathway. In this case, additional
 1166 information can be obtained by reporting flux control ratios based on a reference state which
 1167 indicates stable tissue-mass specific flux. Stereological determination of mitochondrial content
 1168 via two-dimensional transmission electron microscopy can have limitations due to the dynamics
 1169 of mitochondrial size (Meinild Lundby *et al.* 2017). Accurate determination of three-
 1170 dimensional volume by two-dimensional microscopy can be both time consuming and
 1171 statistically challenging (Larsen *et al.* 2012).

1172 The validity of using mitochondrial marker enzymes (citrate synthase activity, Complex
 1173 I–IV amount or activity) for normalization of flux is limited in part by the same factors that
 1174 apply to flux control ratios. Strong correlations between various mitochondrial markers and
 1175 citrate synthase activity (Reichmann *et al.* 1985; Boushel *et al.* 2007; Mogensen *et al.* 2007)
 1176 are expected in a specific tissue of healthy subjects and in disease states not specifically
 1177 targeting citrate synthase. Citrate synthase activity is acutely modifiable by exercise
 1178 (Tonkonogi *et al.* 1997; Leek *et al.* 2001). Evaluation of mitochondrial markers related to a
 1179 selected age and sex cohort cannot be extrapolated to provide recommendations for
 1180 normalization in respirometric diagnosis of disease, in different states of development and
 1181 ageing, different cell types, tissues, and species. mtDNA normalized to nDNA via qPCR is
 1182 correlated to functional mitochondrial markers including OXPHOS- and ET-capacity in some
 1183 cases (Puntschart *et al.* 1995; Wang *et al.* 1999; Menshikova *et al.* 2006; Boushel *et al.* 2007),
 1184 but lack of such correlations have been reported (Menshikova *et al.* 2005; Schultz and Wiesner
 1185 2000; Pesta *et al.* 2011). Several studies indicate a strong correlation between cardiolipin
 1186 content and increase in mitochondrial function with exercise (Menshikova *et al.* 2005;
 1187 Menshikova *et al.* 2007; Larsen *et al.* 2012; Faber *et al.* 2014), but it has not been evaluated as
 1188 a general mitochondrial biomarker in disease.

1189 3.6. Conversion: units

1190
 1191
 1192 Many different units have been used to report the O₂ consumption rate, OCR (**Table 6**).
 1193 SI base units provide the common reference to introduce the theoretical principles (**Figure 6**),
 1194 and are used with appropriately chosen SI prefixes to express numerical data in the most
 1195 practical format, with an effort towards unification within specific areas of application (**Table**

1196 7). Reporting data in *SI* units—including the mole [mol], coulomb [C], joule [J], and second
1197 [s]—should be encouraged, particularly by journals which propose the use of *SI* units.
1198
1199

1200 **Table 6. Conversion of various units used in respirometry and**
1201 **ergometry.** e^- is the number of electrons or reducing equivalents. z_B is the
1202 charge number of entity B.
1203

1 Unit	x	Multiplication factor	<i>SI</i> -unit	Note
ng.atom O·s ⁻¹	(2 e ⁻)	0.5	nmol O ₂ ·s ⁻¹	
ng.atom O·min ⁻¹	(2 e ⁻)	8.33	pmol O ₂ ·s ⁻¹	
natom O·min ⁻¹	(2 e ⁻)	8.33	pmol O ₂ ·s ⁻¹	
nmol O ₂ ·min ⁻¹	(4 e ⁻)	16.67	pmol O ₂ ·s ⁻¹	
nmol O ₂ ·h ⁻¹	(4 e ⁻)	0.2778	pmol O ₂ ·s ⁻¹	
mL O ₂ ·min ⁻¹ at STPD ^a		0.744	μmol O ₂ ·s ⁻¹	1
W = J/s at -470 kJ/mol O ₂		-2.128	μmol O ₂ ·s ⁻¹	
mA = mC·s ⁻¹	(z _{H+} = 1)	10.36	nmol H ⁺ ·s ⁻¹	2
mA = mC·s ⁻¹	(z _{O₂} = 4)	2.59	nmol O ₂ ·s ⁻¹	2
nmol H ⁺ ·s ⁻¹	(z _{H+} = 1)	0.09649	mA	3
nmol O ₂ ·s ⁻¹	(z _{O₂} = 4)	0.38594	mA	3

1204 1 At standard temperature and pressure dry (STPD: 0 °C = 273.15 K and 1 atm =
1205 101.325 kPa = 760 mmHg), the molar volume of an ideal gas, V_m , and V_{m,O_2} is
1206 22.414 and 22.392 L·mol⁻¹, respectively. Rounded to three decimal places, both
1207 values yield the conversion factor of 0.744. For comparison at normal
1208 temperature and pressure dry (NTPD: 20 °C), V_{m,O_2} is 24.038 L·mol⁻¹. Note that
1209 the *SI* standard pressure is 100 kPa.

1210 2 The multiplication factor is $10^6/(z_B \cdot F)$.

1211 3 The multiplication factor is $z_B \cdot F/10^6$.

1212

1213

1214 Although volume is expressed as m³ using the *SI* base unit, the litre [dm³] is a
1215 conventional unit of volume for concentration and is used for most solution chemical kinetics.
1216 If one multiplies $I_{O_2/cell}$ by C_{Ncell} , then the result will not only be the amount of O₂ [mol]
1217 consumed per time [s⁻¹] in one litre [L⁻¹], but also the change in O₂ concentration per second
1218 (for any volume of an ideally closed system). This is ideal for kinetic modeling as it blends with
1219 chemical rate equations where concentrations are typically expressed in mol·L⁻¹ (Wagner *et al.*
1220 2011). In studies of multinuclear cells—such as differentiated skeletal muscle cells—it is easy
1221 to determine the number of nuclei but not the total number of cells. A generalized concept,
1222 therefore, is obtained by substituting cells by nuclei as the sample entity. This does not hold,
1223 however, for enucleated platelets.

1224 For studies of cells, we recommend that respiration be expressed, as far as possible, as:
1225 (1) O₂ flux normalized for a mitochondrial marker, for separation of the effects of mitochondrial
1226 quality and content on cell respiration (this includes *FCRs* as a normalization for a functional
1227 mitochondrial marker); (2) O₂ flux in units of cell volume or mass, for comparison of respiration
1228 of cells with different cell size (Renner *et al.* 2003) and with studies on tissue preparations, and
1229 (3) O₂ flow in units of attomole (10⁻¹⁸ mol) of O₂ consumed in a second by each cell
1230 [amol·s⁻¹·cell⁻¹], numerically equivalent to [pmol·s⁻¹·10⁻⁶ cells]. This convention allows
1231 information to be easily used when designing experiments in which O₂ flow must be considered.
1232 For example, to estimate the volume-specific O₂ flux in an instrument chamber that would be

1233 expected at a particular cell number concentration, one simply needs to multiply the flow per
 1234 cell by the number of cells per volume of interest. This provides the amount of O₂ [mol]
 1235 consumed per time [s⁻¹] per unit volume [L⁻¹]. At an O₂ flow of 100 amol·s⁻¹·cell⁻¹ and a cell
 1236 density of 10⁹ cells·L⁻¹ (10⁶ cells·mL⁻¹), the volume-specific O₂ flux is 100 nmol·s⁻¹·L⁻¹ (100
 1237 pmol·s⁻¹·mL⁻¹).
 1238
 1239

Table 7. Conversion of units with preservation of numerical values.

Name	Frequently used unit	Equivalent unit	Note
volume-specific flux, J_{V,O_2}	pmol·s ⁻¹ ·mL ⁻¹ mmol·s ⁻¹ ·L ⁻¹	nmol·s ⁻¹ ·L ⁻¹ mol·s ⁻¹ ·m ⁻³	1
cell-specific flow, $I_{O_2/cell}$	pmol·s ⁻¹ ·10 ⁻⁶ cells	amol·s ⁻¹ ·cell ⁻¹	2
	pmol·s ⁻¹ ·10 ⁻⁹ cells	zmol·s ⁻¹ ·cell ⁻¹	3
cell number concentration, C_{Nce}	10 ⁶ cells·mL ⁻¹	10 ⁹ cells·L ⁻¹	
mitochondrial protein concentration, C_{mtE}	0.1 mg·mL ⁻¹	0.1 g·L ⁻¹	
mass-specific flux, $J_{O_2/m}$	pmol·s ⁻¹ ·mg ⁻¹	nmol·s ⁻¹ ·g ⁻¹	4
catabolic power, P_k	μW·10 ⁻⁶ cells	pW·cell ⁻¹	1
volume	1,000 L	m ³ (1,000 kg)	
	L	dm ³ (kg)	
	mL	cm ³ (g)	
	μL	mm ³ (mg)	
	fL	μm ³ (pg)	5
amount of substance concentration	M = mol·L ⁻¹	mol·dm ⁻³	

1240

1241 1 pmol: picomole = 10⁻¹² mol1242 2 amol: attomole = 10⁻¹⁸ mol1243 3 zmol: zeptomole = 10⁻²¹ mol

1244

1245 ET-capacity in human cell types including HEK 293, primary HUVEC and fibroblasts
 1246 ranges from 50 to 180 amol·s⁻¹·cell⁻¹, measured in intact cells in the noncoupled state (see
 1247 Gnaiger 2014). At 100 amol·s⁻¹·cell⁻¹ corrected for *Rox*, the current across the mt-membranes,
 1248 I_{H^+e} , approximates 193 pA·cell⁻¹ or 0.2 nA per cell. See Rich (2003) for an extension of
 1249 quantitative bioenergetics from the molecular to the human scale, with a transmembrane proton
 1250 flux equivalent to 520 A in an adult at a catabolic power of -110 W. Modelling approaches
 1251 illustrate the link between protonmotive force and currents (Willis *et al.* 2016).

1252 We consider isolated mitochondria as powerhouses and proton pumps as molecular
 1253 machines to relate experimental results to energy metabolism of the intact cell. The cellular
 1254 P_»/O₂ based on oxidation of glycogen is increased by the glycolytic (fermentative) substrate-
 1255 level phosphorylation of 3 P_»/Glyc or 0.5 mol P_» for each mol O₂ consumed in the complete
 1256 oxidation of a mol glycosyl unit (Glyc). Adding 0.5 to the mitochondrial P_»/O₂ ratio of 5.4
 1257 yields a bioenergetic cell physiological P_»/O₂ ratio close to 6. Two NADH equivalents are
 1258 formed during glycolysis and transported from the cytosol into the mitochondrial matrix, either
 1259 by the malate-aspartate shuttle or by the glycerophosphate shuttle (**Figure 1**) resulting in
 1260 different theoretical yields of ATP generated by mitochondria, the energetic cost of which
 1261 potentially must be taken into account. Considering also substrate-level phosphorylation in the
 1262 TCA cycle, this high P_»/O₂ ratio not only reflects proton translocation and OXPHOS studied
 1263 in isolation, but integrates mitochondrial physiology with energy transformation in the living
 1264 cell (Gnaiger 1993a).
 1265
 1266

4. Conclusions

MitoEAGLE can serve as a gateway to better diagnose mitochondrial respiratory defects linked to genetic variation, age-related health risks, sex-specific mitochondrial performance, lifestyle with its effects on degenerative diseases, and thermal and chemical environment. The present recommendations on coupling control states and rates, linked to the concept of the protonmotive force, are focused on studies with mitochondrial preparations. These will be extended in a series of reports on pathway control of mitochondrial respiration, respiratory states in intact cells, and harmonization of experimental procedures.

OXPHOS analysis is based on the study of mitochondrial preparations complementary to bioenergetic investigations of intact cells and organisms—from animal models to healthy persons or patients. Metabolic fluxes measured in defined coupling and pathway control states provide insights into the meaning of cellular and organismic respiration. An O_2 flux balance scheme illustrates the relationships and general definitions (**Box 3**).

Box 3: Definitions: mitochondrial and cell respiration

Mitochondrial respiration with reduction of oxygen catalysed by the electron transfer system (catabolic, *a*), catabolic respiration (including non-mitochondrial oxidation reactions, *b*), and oxygen balance of internal (*c*) and external (*d*) respiration

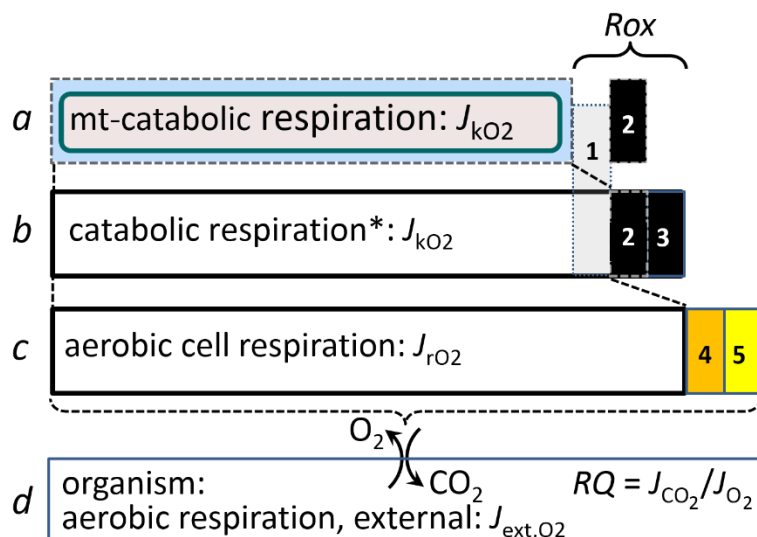
All chemical reactions, r , that consume O_2 in the cells of an organism, contribute to cell respiration, J_{rO_2} . (1) Non-mitochondrial contribution to O_2 consumption by catabolic reactions, particularly

peroxisomal oxidases (* the reactions k have to be defined specifically for *a* and *b*; **Figure 1**); (2) mitochondrial residual oxygen consumption, Rox , after blocking the electron transfer system; (3) non-mitochondrial Rox ; (4) extracellular O_2 consumption; (5) aerobic microbial respiration. Bars are not at a quantitative scale.

a Mitochondrial catabolic respiration, J_{kO_2} , is the O_2 consumption by the ETS (**Figure 2**), excluding Rox .

b Catabolic respiration, J_{kO_2} , is the O_2 consumption associated with catabolic pathways in the cell, including mitochondrial and peroxisomal oxidation reactions.

c Aerobic cell respiration, J_{rO_2} , takes into account internal O_2 -consuming reactions, r , including Rox . In aerobic cell respiration, redox balance is maintained by the use of O_2 as electron acceptor. Internal respiration of an organism includes extracellular O_2 consumption and aerobic respiration by the microbiome. In general, respiration is distinguished from fermentation by: (1) the use of external electron acceptors for the maintenance of redox balance, whereas fermentation is characterized by the use of an internal electron acceptor produced in intermediary metabolism; and (2) compartmental coupling in vectorial oxidative phosphorylation, in contrast to exclusively scalar substrate-level phosphorylation in fermentation.



1317 **d External respiration** balances internal respiration at steady-state, with circulation of the
 1318 externally exchanged O₂ between tissues and diffusion across cell membranes. O₂ is
 1319 transported from the environment across the respiratory cascade to the intracellular
 1320 compartment, while bicarbonate and CO₂ are transported in reverse to the extracellular
 1321 milieu and the organismic environment. Hemoglobin provides the molecular paradigm for
 1322 the combination of O₂ and CO₂ exchange, as do lungs and gills on the morphological
 1323 level. The respiratory quotient, *RQ*, is the molar CO₂/O₂ exchange ratio; when combined
 1324 with the respiratory nitrogen quotient, N/O₂, the *RQ* reflects the proportion of
 1325 carbohydrate, lipid and protein utilized in cell respiration during aerobically balanced
 1326 steady-states.

1327
 1328 Cell respiration is the process of exergonic and exothermic energy transformation in
 1329 which scalar redox reactions are coupled to vectorial ion translocation across a semipermeable
 1330 membrane, which separates the small volume of a bacterial cell or mitochondrion from the
 1331 larger volume of its surroundings. The electrochemical exergy can be partially conserved in the
 1332 phosphorylation of ADP to ATP or in ion pumping, or dissipated in an electrochemical short-
 1333 circuit. Respiration is thus clearly distinguished from fermentation as the counterpart of cellular
 1334 core energy metabolism. Respiration is separated in mitochondrial preparations from the
 1335 interactions with the fermentative pathways of the intact cell.

1336 The optimal choice for expressing mitochondrial and cell respiration as O₂ flow per
 1337 biological sample, and normalization for specific tissue-markers (volume, mass, protein) and
 1338 mitochondrial markers (volume, protein, content, mtDNA, activity of marker enzymes,
 1339 respiratory reference state) is guided by the scientific question under study. Interpretation of
 1340 the data depends critically on appropriate normalization.

1341 We recommend for studies with mitochondrial preparations:

- 1342 • Normalization of respiratory rates should be provided as far as possible: (1) biophysical
 1343 normalization: on a per cell basis as O₂ flow (may not be possible when dealing with
 1344 tissues); (2) cellular normalization: per g cell or tissue protein, or per cell or tissue mass
 1345 as mass-specific O₂ flux; and (3) mitochondrial normalization: per mitochondrial marker
 1346 as mt-specific flux. With information on cell size and the use of multiple normalizations,
 1347 maximum potential information is available (Renner *et al.* 2003; Wagner *et al.* 2011;
 1348 Gnaiger 2014). Reporting flow in a respiratory chamber [nmol·s⁻¹] is discouraged, since
 1349 it restricts the analysis to intra-experimental comparison of relative (qualitative)
 1350 differences.
- 1351 • Catabolic mitochondrial respiration is distinguished from residual oxygen consumption.
 1352 Fluxes in mitochondrial coupling states should be, as far as possible, corrected for residual
 1353 oxygen consumption.
- 1354 • In studies of isolated mitochondria, the mitochondrial recovery and yield should be
 1355 reported. Experimental criteria for evaluation of purity versus integrity should be
 1356 considered. Mitochondrial markers—such as citrate synthase activity as an enzymatic
 1357 matrix marker—provide a link to the tissue of origin on the basis of calculating the
 1358 mitochondrial recovery, *i.e.*, the fraction of mitochondrial marker obtained from a unit
 1359 mass of tissue. Total mitochondrial protein is frequently applied as a mitochondrial
 1360 marker, which is restricted to isolated mitochondria.
- 1361 • In studies of permeabilized cells, the viability of the cell culture or cell suspension of
 1362 origin should be reported. Normalization should be evaluated for total cell count or viable
 1363 cell count.
- 1364 • Terms and symbols are summarized in **Table 8**. Their use will facilitate transdisciplinary
 1365 communication and support further developments towards a consistent theory of
 1366 bioenergetics and mitochondrial physiology.

- 1367 • Technical terms related to and defined with normal words can be used as index terms in
 1368 databases, support the creation of ontologies towards semantic information processing
 1369 (MitoPedia), and help in communicating analytical findings as impactful data-driven
 1370 stories. ‘*Making data available without making it understandable may be worse than not*
 1371 *making it available at all*’ (National Academies of Sciences, Engineering, and Medicine
 1372 2018). Success will depend on taking next steps: (1) exhaustive text-mining considering
 1373 Omics data and functional data; (2) network analysis of Omics data with bioinformatics
 1374 tools; (3) cross-validation with distinct bioinformatics approaches; (4) correlation with
 1375 functional data; (5) guidelines for biological validation of network data. This is a call to
 1376 carefully contribute to FAIR principles (Findable, Accessible, Interoperable, Reusable)
 1377 for the sharing of scientific data.

1379 **Table 8. Terms, symbols, and units.**
 1380
 1381

1382 Term	1383 Symbol	1384 Unit	1385 Links and comments
1386 alternative quinol oxidase	1387 AOX		1388 Figure 2A
1389 amount of substance B	1390 n_B	1391 [mol]	
1392 ATP yield per O ₂	1393 Y_{P/O_2}		1394 P _» /O ₂ ratio measured in any respiratory 1395 state
1396 catabolic reaction	1397 k		1398 Figure 2, Box 3
1399 catabolic respiration	1400 J_{kO_2}	1401 <i>varies</i>	1402 Figure 2, Box 3
1403 cell number	1404 N_{cell}	1405 [x]	1406 Table 5; $N_{cell} = N_{vce} + N_{dce}$
1407 cell respiration	1408 J_{rO_2}	1409 <i>varies</i>	1410 Box 3
1411 cell viability index	1412 CVI		1413 $CVI = N_{vce}/N_{cell} = 1 - N_{dce}/N_{cell}$
1414 Complexes I to IV	1415 CI to CIV		1416 respiratory ET Complexes; Figure 2A
1417 concentration of substance B	1418 $c_B = n_B \cdot V^{-1}$; [B]	1419 [mol·m ⁻³]	1420 Box 2
1421 dead cell number	1422 N_{dce}	1423 [x]	1424 Table 5; non-viable cells, loss of plasma 1425 membrane barrier function
1426 electron transfer system	1427 ETS		1428 Figure 2A, Figure 4
1429 flow, for substance B	1430 I_B	1431 [mol·s ⁻¹]	1432 system-related extensive quantity; 1433 Figure 6
1434 flux, for substance B	1435 J_B	1436 <i>varies</i>	1437 size-specific quantity; Figure 6
1438 inorganic phosphate	1439 P _i		1440 Figure 2C
1441 intact cell number, viable cell number	1442 N_{vce}	1443 [x]	1444 Table 5; viable cells, intact of plasma 1445 membrane barrier function
1446 LEAK	1447 LEAK		1448 Table 1, Figure 4
1449 mass of sample X	1450 m_X	1451 [kg]	1452 Table 4
1453 mass of entity X	1454 M_X	1455 [kg]	1456 mass of object X; Table 4
1457 MITOCARTA			1458 https://www.broadinstitute.org/scientific-community/science/programs/metabolic-disease-program/publications/mitocarta/mitocarta-in-0
1459 MitoPedia			1460 http://www.bioblast.at/index.php/MitoPedia
1461 mitochondria or mitochondrial	1462 mt		1463 Box 1
1464 mitochondrial DNA	1465 mtDNA		1466 Box 1
1467 mitochondrial concentration	1468 $C_{mtE} = mtE \cdot V^{-1}$	1469 [mtEU·m ⁻³]	1470 Table 4
1471 mitochondrial content	1472 $mtE_X = mtE \cdot N_X^{-1}$	1473 [mtEU·x ⁻¹]	1474 Table 4
1475 mitochondrial elemental unit	1476 mtEU	1477 <i>varies</i>	1478 Table 4, specific units for mt-marker
1479 mitochondrial inner membrane	1480 mtIM		1481 Figure 1; MIM is widely used; the first 1482 M is replaced by mt; Box 1
1483 mitochondrial outer membrane	1484 mtOM		1485 Figure 1; MOM is widely used; the first 1486 M is replaced by mt; Box 1
1487 mitochondrial recovery	1488 Y_{mtE}		1489 fraction of <i>mtE</i> recovered in sample 1490 from the tissue of origin
1491 mitochondrial yield	1492 $Y_{mtE/m}$		1493 $Y_{mtE/m} = Y_{mtE} \cdot D_{mtE}$

1426	negative	neg		Figure 2C
1427	number concentration of X	C_{NX}	$[x \cdot m^{-3}]$	Table 4
1428	number of entities X	N_X	$[x]$	Table 4, Figure 7
1429	number of entity B	N_B	$[x]$	Table 4
1430	oxidative phosphorylation	OXPPOS		Table 1, Figure 4
1431	oxygen concentration	$c_{O_2} = n_{O_2} \cdot V^{-1}$; $[O_2]$	$[mol \cdot m^{-3}]$	Section 3.2
1432	oxygen flux, in reaction r	J_{rO_2}	<i>varies</i>	Box 3
1433	permeabilized cell number	N_{pcc}	$[x]$	Table 5; experimental permeabilization of plasma membrane; $N_{pcc} = N_{cell}$
1434				
1435	phosphorylation of ADP to ATP	$P \gg$		Section 2.2
1436	positive	pos		Figure 2C
1437	proton in the negative compartment	H^{+neg}		Figure 2C
1438	proton in the positive compartment	H^{+pos}		Figure 2C
1439	rate of electron transfer in ET state	E		ET-capacity; Table 1
1440	rate of LEAK respiration	L		Table 1
1441	rate of oxidative phosphorylation	P		OXPPOS capacity; Table 1
1442	rate of residual oxygen consumption	ROx		Table 1
1443	residual oxygen consumption	ROX		Table 1
1444	respiratory supercomplex	$SC I_n III_n IV_n$		Box 1; supramolecular assemblies composed of variable copy numbers (n) of CI, CIII and CIV
1445				
1446				
1447	specific mitochondrial density	$D_{mtE} = mtE \cdot m_X^{-1}$	$[mtEU \cdot kg^{-1}]$	Table 4
1448	volume	V	$[m^3]$	Table 7
1449	weight, dry weight	W_d	$[kg]$	used as mass of sample X ; Figure 6
1450	weight, wet weight	W_w	$[kg]$	used as mass of sample X ; Figure 6
1451				

1452

1453

1454 Acknowledgements

1455 We thank M. Beno for management assistance. Supported by COST Action CA15203
1456 MitoEAGLE and K-Regio project MitoFit (E.G.).

1457

1458 **Competing financial interests:** E.G. is founder and CEO of Oroboros Instruments, Innsbruck,
1459 Austria.

1460

1461

1462 5. References

1463

1464 Altmann R (1894) Die Elementarorganismen und ihre Beziehungen zu den Zellen. Zweite vermehrte Auflage.

1465 Verlag Von Veit & Comp, Leipzig:160 pp.

1466 Beard DA (2005) A biophysical model of the mitochondrial respiratory system and oxidative phosphorylation.

1467 PLoS Comput Biol 1(4):e36.

1468 Benda C (1898) Weitere Mitteilungen über die Mitochondria. Verh Dtsch Physiol Ges:376-83.

1469 Birkedal R, Laasmaa M, Vendelin M (2014) The location of energetic compartments affects energetic

1470 communication in cardiomyocytes. Front Physiol 5:376.

1471 Breton S, Beaupré HD, Stewart DT, Hoeh WR, Blier PU (2007) The unusual system of doubly uniparental

1472 inheritance of mtDNA: isn't one enough? Trends Genet 23:465-74.

1473 Brown GC (1992) Control of respiration and ATP synthesis in mammalian mitochondria and cells. Biochem J

1474 284:1-13.

1475 Calvo SE, Klauser CR, Mootha VK (2016) MitoCarta2.0: an updated inventory of mammalian mitochondrial

1476 proteins. Nucleic Acids Research 44:D1251-7.

1477 Calvo SE, Julien O, Clauser KR, Shen H, Kamer KJ, Wells JA, Mootha VK (2017) Comparative analysis of

1478 mitochondrial N-termini from mouse, human, and yeast. Mol Cell Proteomics 16:512-23.

1479 Campos JC, Queliconi BB, Bozi LHM, Bechara LRG, Dourado PMM, Andres AM, Jannig PR, Gomes KMS,

1480 Zambelli VO, Rocha-Resende C, Guatimosim S, Brum PC, Mochly-Rosen D, Gottlieb RA, Kowaltowski AJ,

1481 Ferreira JCB (2017) Exercise reestablishes autophagic flux and mitochondrial quality control in heart failure.

1482 Autophagy 13:1304-317.

1483 Canton M, Luvisetto S, Schmehl I, Azzone GF (1995) The nature of mitochondrial respiration and

1484 discrimination between membrane and pump properties. Biochem J 310:477-81.

- 1485 Chance B, Williams GR (1955a) Respiratory enzymes in oxidative phosphorylation. I. Kinetics of oxygen
1486 utilization. *J Biol Chem* 217:383-93.
- 1487 Chance B, Williams GR (1955b) Respiratory enzymes in oxidative phosphorylation: III. The steady state. *J Biol*
1488 *Chem* 217:409-27.
- 1489 Chance B, Williams GR (1955c) Respiratory enzymes in oxidative phosphorylation. IV. The respiratory chain. *J*
1490 *Biol Chem* 217:429-38.
- 1491 Chance B, Williams GR (1956) The respiratory chain and oxidative phosphorylation. *Adv Enzymol Relat Subj*
1492 *Biochem* 17:65-134.
- 1493 Cobb LJ, Lee C, Xiao J, Yen K, Wong RG, Nakamura HK, Mehta HH, Gao Q, Ashur C, Huffman DM, Wan J,
1494 Muzumdar R, Barzilai N, Cohen P (2016) Naturally occurring mitochondrial-derived peptides are age-
1495 dependent regulators of apoptosis, insulin sensitivity, and inflammatory markers. *Aging (Albany NY)* 8:796-
1496 809.
- 1497 Cohen ER, Cvitas T, Frey JG, Holmström B, Kuchitsu K, Marquardt R, Mills I, Pavese F, Quack M, Stohner J,
1498 Strauss HL, Takami M, Thor HL (2008) Quantities, units and symbols in physical chemistry, IUPAC Green
1499 Book, 3rd Edition, 2nd Printing, IUPAC & RSC Publishing, Cambridge.
- 1500 Cooper H, Hedges LV, Valentine JC, eds (2009) The handbook of research synthesis and meta-analysis. Russell
1501 Sage Foundation.
- 1502 Coopersmith J (2010) Energy, the subtle concept. The discovery of Feynman's blocks from Leibnitz to Einstein.
1503 Oxford University Press:400 pp.
- 1504 Cummins J (1998) Mitochondrial DNA in mammalian reproduction. *Rev Reprod* 3:172-82.
- 1505 Dai Q, Shah AA, Garde RV, Yonish BA, Zhang L, Medvitz NA, Miller SE, Hansen EL, Dunn CN, Price TM
1506 (2013) A truncated progesterone receptor (PR-M) localizes to the mitochondrion and controls cellular
1507 respiration. *Mol Endocrinol* 27:741-53.
- 1508 Divakaruni AS, Brand MD (2011) The regulation and physiology of mitochondrial proton leak. *Physiology*
1509 (Bethesda) 26:192-205.
- 1510 Doerrier C, Garcia-Souza LF, Krumschnabel G, Wohlfarter Y, Mészáros AT, Gnaiger E (2018) High-Resolution
1511 FluoRespirometry and OXPHOS protocols for human cells, permeabilized fibres from small biopsies of
1512 muscle and isolated mitochondria. *Methods Mol. Biol.* (in press)
- 1513 Doskey CM, van 't Erve TJ, Wagner BA, Buettner GR (2015) Moles of a substance per cell is a highly
1514 informative dosing metric in cell culture. *PLOS ONE* 10:e0132572.
- 1515 Drahotová Z, Milerová M, Stieglerová A, Houstek J, Ostádal B (2004) Developmental changes of cytochrome *c*
1516 oxidase and citrate synthase in rat heart homogenate. *Physiol Res* 53:119-22.
- 1517 Duarte FV, Palmeira CM, Rolo AP (2014) The role of microRNAs in mitochondria: small players acting wide.
1518 *Genes (Basel)* 5:865-86.
- 1519 Ernster L, Schatz G (1981) Mitochondria: a historical review. *J Cell Biol* 91:227s-55s.
- 1520 Estabrook RW (1967) Mitochondrial respiratory control and the polarographic measurement of ADP:O ratios.
1521 *Methods Enzymol* 10:41-7.
- 1522 Faber C, Zhu ZJ, Castellino S, Wagner DS, Brown RH, Peterson RA, Gates L, Barton J, Bickett M, Hagerty L,
1523 Kimbrough C, Sola M, Bailey D, Jordan H, Elangbam CS (2014) Cardiolipin profiles as a potential
1524 biomarker of mitochondrial health in diet-induced obese mice subjected to exercise, diet-restriction and
1525 ephedrine treatment. *J Appl Toxicol* 34:1122-9.
- 1526 Fell D (1997) Understanding the control of metabolism. Portland Press.
- 1527 Garlid KD, Beavis AD, Ratkje SK (1989) On the nature of ion leaks in energy-transducing membranes. *Biochim*
1528 *Biophys Acta* 976:109-20.
- 1529 Garlid KD, Semrad C, Zinchenko V. Does redox slip contribute significantly to mitochondrial respiration? In:
1530 Schuster S, Rigoulet M, Ouhabi R, Mazat J-P, eds (1993) Modern trends in biothermokinetics. Plenum Press,
1531 New York, London:287-93.
- 1532 Gerö D, Szabo C (2016) Glucocorticoids suppress mitochondrial oxidant production via upregulation of
1533 uncoupling protein 2 in hyperglycemic endothelial cells. *PLoS One* 11:e0154813.
- 1534 Gnaiger E. Efficiency and power strategies under hypoxia. Is low efficiency at high glycolytic ATP production a
1535 paradox? In: *Surviving Hypoxia: Mechanisms of Control and Adaptation*. Hochachka PW, Lutz PL, Sick T,
1536 Rosenthal M, Van den Thillart G, eds (1993a) CRC Press, Boca Raton, Ann Arbor, London, Tokyo:77-109.
- 1537 Gnaiger E (1993b) Nonequilibrium thermodynamics of energy transformations. *Pure Appl Chem* 65:1983-2002.
- 1538 Gnaiger E (2001) Bioenergetics at low oxygen: dependence of respiration and phosphorylation on oxygen and
1539 adenosine diphosphate supply. *Respir Physiol* 128:277-97.
- 1540 Gnaiger E (2009) Capacity of oxidative phosphorylation in human skeletal muscle. New perspectives of
1541 mitochondrial physiology. *Int J Biochem Cell Biol* 41:1837-45.
- 1542 Gnaiger E (2014) Mitochondrial pathways and respiratory control. An introduction to OXPHOS analysis. 4th ed.
1543 *Mitochondr Physiol Network* 19.12. Oroboros MiPNet Publications, Innsbruck:80 pp.
- 1544 Gnaiger E, Méndez G, Hand SC (2000) High phosphorylation efficiency and depression of uncoupled respiration
1545 in mitochondria under hypoxia. *Proc Natl Acad Sci USA* 97:11080-5.

- 1546 Greggio C, Jha P, Kulkarni SS, Lagarrigue S, Broskey NT, Boutant M, Wang X, Conde Alonso S, Ofori E,
 1547 Auwerx J, Cantó C, Amati F (2017) Enhanced respiratory chain supercomplex formation in response to
 1548 exercise in human skeletal muscle. *Cell Metab* 25:301-11.
- 1549 Hinkle PC (2005) P/O ratios of mitochondrial oxidative phosphorylation. *Biochim Biophys Acta* 1706:1-11.
- 1550 Hofstadter DR (1979) Gödel, Escher, Bach: An eternal golden braid. A metaphorical fugue on minds and
 1551 machines in the spirit of Lewis Carroll. Harvester Press:499 pp.
- 1552 Illaste A, Laasmaa M, Peterson P, Vendelin M (2012) Analysis of molecular movement reveals latticelike
 1553 obstructions to diffusion in heart muscle cells. *Biophys J* 102:739-48.
- 1554 Jasienski M, Bazzaz FA (1999) The fallacy of ratios and the testability of models in biology. *Oikos* 84:321-26.
- 1555 Jepihina N, Beraud N, Sepp M, Birkedal R, Vendelin M (2011) Permeabilized rat cardiomyocyte response
 1556 demonstrates intracellular origin of diffusion obstacles. *Biophys J* 101:2112-21.
- 1557 Klepinin A, Ounpuu L, Guzun R, Chekulayev V, Timohhina N, Tepp K, Shevchuk I, Schlattner U, Kaambre T
 1558 (2016) Simple oxygraphic analysis for the presence of adenylate kinase 1 and 2 in normal and tumor cells. *J*
 1559 *Bioenerg Biomembr* 48:531-48.
- 1560 Klingenberg M (2017) UCPI - A sophisticated energy valve. *Biochimie* 134:19-27.
- 1561 Koit A, Shevchuk I, Ounpuu L, Klepinin A, Chekulayev V, Timohhina N, Tepp K, Puurand M, Truu L, Heck K,
 1562 Valvere V, Guzun R, Kaambre T (2017) Mitochondrial respiration in human colorectal and breast cancer
 1563 clinical material is regulated differently. *Oxid Med Cell Longev* 1372640.
- 1564 Komlódi T, Tretter L (2017) Methylene blue stimulates substrate-level phosphorylation catalysed by succinyl-
 1565 CoA ligase in the citric acid cycle. *Neuropharmacology* 123:287-98.
- 1566 Lane N (2005) Power, sex, suicide: mitochondria and the meaning of life. Oxford University Press:354 pp.
- 1567 Larsen S, Nielsen J, Neigaard Nielsen C, Nielsen LB, Wibrand F, Stride N, Schroder HD, Boushel RC, Helge
 1568 JW, Dela F, Hey-Mogensen M (2012) Biomarkers of mitochondrial content in skeletal muscle of healthy
 1569 young human subjects. *J Physiol* 590:3349-60.
- 1570 Lee C, Zeng J, Drew BG, Sallam T, Martin-Montalvo A, Wan J, Kim SJ, Mehta H, Hevener AL, de Cabo R,
 1571 Cohen P (2015) The mitochondrial-derived peptide MOTS-c promotes metabolic homeostasis and reduces
 1572 obesity and insulin resistance. *Cell Metab* 21:443-54.
- 1573 Lee SR, Kim HK, Song IS, Youm J, Dizon LA, Jeong SH, Ko TH, Heo HJ, Ko KS, Rhee BD, Kim N, Han J
 1574 (2013) Glucocorticoids and their receptors: insights into specific roles in mitochondria. *Prog Biophys Mol*
 1575 *Biol* 112:44-54.
- 1576 Leek BT, Mudaliar SR, Henry R, Mathieu-Costello O, Richardson RS (2001) Effect of acute exercise on citrate
 1577 synthase activity in untrained and trained human skeletal muscle. *Am J Physiol Regul Integr Comp Physiol*
 1578 280:R441-7.
- 1579 Lemieux H, Blier PU, Gnaiger E (2017) Remodeling pathway control of mitochondrial respiratory capacity by
 1580 temperature in mouse heart: electron flow through the Q-junction in permeabilized fibers. *Sci Rep* 7:2840.
- 1581 Lenaz G, Tioli G, Falasca AI, Genova ML (2017) Respiratory supercomplexes in mitochondria. In: *Mechanisms*
 1582 *of primary energy trasduction in biology*. M Wikstrom (ed) Royal Society of Chemistry Publishing, London,
 1583 UK:296-337.
- 1584 Margulis L (1970) Origin of eukaryotic cells. New Haven: Yale University Press.
- 1585 Meinild Lundby AK, Jacobs RA, Gehrig S, de Leur J, Hauser M, Bonne TC, Flück D, Dandanell S, Kirk N,
 1586 Kaech A, Ziegler U, Larsen S, Lundby C (2018) Exercise training increases skeletal muscle mitochondrial
 1587 volume density by enlargement of existing mitochondria and not de novo biogenesis. *Acta Physiol* 222,
 1588 e12905.
- 1589 Menshikova EV, Ritov VB, Fairfull L, Ferrell RE, Kelley DE, Goodpaster BH (2006) Effects of exercise on
 1590 mitochondrial content and function in aging human skeletal muscle. *J Gerontol A Biol Sci Med Sci* 61:534-
 1591 40.
- 1592 Menshikova EV, Ritov VB, Ferrell RE, Azuma K, Goodpaster BH, Kelley DE (2007) Characteristics of skeletal
 1593 muscle mitochondrial biogenesis induced by moderate-intensity exercise and weight loss in obesity. *J Appl*
 1594 *Physiol* (1985) 103:21-7.
- 1595 Menshikova EV, Ritov VB, Toledo FG, Ferrell RE, Goodpaster BH, Kelley DE (2005) Effects of weight loss
 1596 and physical activity on skeletal muscle mitochondrial function in obesity. *Am J Physiol Endocrinol Metab*
 1597 288:E818-25.
- 1598 Miller GA (1991) The science of words. Scientific American Library New York:276 pp.
- 1599 Mitchell P (1961) Coupling of phosphorylation to electron and hydrogen transfer by a chemi-osmotic type of
 1600 mechanism. *Nature* 191:144-8.
- 1601 Mitchell P (2011) Chemiosmotic coupling in oxidative and photosynthetic phosphorylation. *Biochim Biophys*
 1602 *Acta Bioenergetics* 1807:1507-38.
- 1603 Mogensen M, Sahlin K, Fernström M, Glintborg D, Vind BF, Beck-Nielsen H, Højlund K (2007) Mitochondrial
 1604 respiration is decreased in skeletal muscle of patients with type 2 diabetes. *Diabetes* 56:1592-9.
- 1605 Mohr PJ, Phillips WD (2015) Dimensionless units in the SI. *Metrologia* 52:40-7.
- 1606 Moreno M, Giacco A, Di Munno C, Goglia F (2017) Direct and rapid effects of 3,5-diiodo-L-thyronine (T2).
 1607 *Mol Cell Endocrinol* 7207:30092-8.

- 1608 Morrow RM, Picard M, Derbeneva O, Leipzig J, McManus MJ, Gousspillou G, Barbat-Artigas S, Dos Santos C,
1609 Hepple RT, Murdock DG, Wallace DC (2017) Mitochondrial energy deficiency leads to hyperproliferation of
1610 skeletal muscle mitochondria and enhanced insulin sensitivity. *Proc Natl Acad Sci U S A* 114:2705-10.
- 1611 Murley A, Nunnari J (2016) The emerging network of mitochondria-organelle contacts. *Mol Cell* 61:648-53.
- 1612 National Academies of Sciences, Engineering, and Medicine (2018) International coordination for science data
1613 infrastructure: Proceedings of a workshop—in brief. Washington, DC: The National Academies Press. doi:
1614 <https://doi.org/10.17226/25015>.
- 1615 Paradies G, Paradies V, De Benedictis V, Ruggiero FM, Petrosillo G (2014) Functional role of cardiolipin in
1616 mitochondrial bioenergetics. *Biochim Biophys Acta* 1837:408-17.
- 1617 Pesta D, Gnaiger E (2012) High-Resolution Respirometry. OXPHOS protocols for human cells and
1618 permeabilized fibres from small biopsies of human muscle. *Methods Mol Biol* 810:25-58.
- 1619 Pesta D, Hoppel F, Macek C, Messner H, Faulhaber M, Kobel C, Parson W, Burtcher M, Schocke M, Gnaiger
1620 E (2011) Similar qualitative and quantitative changes of mitochondrial respiration following strength and
1621 endurance training in normoxia and hypoxia in sedentary humans. *Am J Physiol Regul Integr Comp Physiol*
1622 301:R1078–87.
- 1623 Price TM, Dai Q (2015) The role of a mitochondrial progesterone receptor (PR-M) in progesterone action.
1624 *Semin Reprod Med* 33:185-94.
- 1625 Puchowicz MA, Varnes ME, Cohen BH, Friedman NR, Kerr DS, Hoppel CL (2004) Oxidative phosphorylation
1626 analysis: assessing the integrated functional activity of human skeletal muscle mitochondria – case studies.
1627 *Mitochondrion* 4:377-85. Puntschart A, Claassen H, Jostarndt K, Hoppeler H, Billeter R (1995) mRNAs of
1628 enzymes involved in energy metabolism and mtDNA are increased in endurance-trained athletes. *Am J*
1629 *Physiol* 269:C619-25.
- 1630 Quiros PM, Mottis A, Auwerx J (2016) Mitonuclear communication in homeostasis and stress. *Nat Rev Mol*
1631 *Cell Biol* 17:213-26.
- 1632 Rackham O, Mercer TR, Filipovska A (2012) The human mitochondrial transcriptome and the RNA-binding
1633 proteins that regulate its expression. *WIREs RNA* 3:675–95.
- 1634 Reichmann H, Hoppeler H, Mathieu-Costello O, von Bergen F, Pette D (1985) Biochemical and ultrastructural
1635 changes of skeletal muscle mitochondria after chronic electrical stimulation in rabbits. *Pflügers Arch* 404:1-
1636 9.
- 1637 Renner K, Amberger A, Konwalinka G, Gnaiger E (2003) Changes of mitochondrial respiration, mitochondrial
1638 content and cell size after induction of apoptosis in leukemia cells. *Biochim Biophys Acta* 1642:115-23.
- 1639 Rich P (2003) Chemiosmotic coupling: The cost of living. *Nature* 421:583.
- 1640 Rostovtseva TK, Sheldon KL, Hassanzadeh E, Monge C, Saks V, Bezrukov SM, Sackett DL (2008) Tubulin
1641 binding blocks mitochondrial voltage-dependent anion channel and regulates respiration. *Proc Natl Acad Sci*
1642 *USA* 105:18746-51.
- 1643 Rustin P, Parfait B, Chretien D, Bourgeron T, Djouadi F, Bastin J, Rötig A, Munnich A (1996) Fluxes of
1644 nicotinamide adenine dinucleotides through mitochondrial membranes in human cultured cells. *J Biol Chem*
1645 271:14785-90.
- 1646 Saks VA, Veksler VI, Kuznetsov AV, Kay L, Sikk P, Tiivel T, Tranqui L, Olivares J, Winkler K, Wiedemann F,
1647 Kunz WS (1998) Permeabilised cell and skinned fiber techniques in studies of mitochondrial function in
1648 vivo. *Mol Cell Biochem* 184:81-100.
- 1649 Salabei JK, Gibb AA, Hill BG (2014) Comprehensive measurement of respiratory activity in permeabilized cells
1650 using extracellular flux analysis. *Nat Protoc* 9:421-38.
- 1651 Sazanov LA (2015) A giant molecular proton pump: structure and mechanism of respiratory complex I. *Nat Rev*
1652 *Mol Cell Biol* 16:375-88.
- 1653 Schneider TD (2006) Claude Shannon: biologist. The founder of information theory used biology to formulate
1654 the channel capacity. *IEEE Eng Med Biol Mag* 25:30-3.
- 1655 Schönfeld P, Dymkowska D, Wojtczak L (2009) Acyl-CoA-induced generation of reactive oxygen species in
1656 mitochondrial preparations is due to the presence of peroxisomes. *Free Radic Biol Med* 47:503-9.
- 1657 Schultz J, Wiesner RJ (2000) Proliferation of mitochondria in chronically stimulated rabbit skeletal muscle--
1658 transcription of mitochondrial genes and copy number of mitochondrial DNA. *J Bioenerg Biomembr* 32:627-
1659 34.
- 1660 Speijer D (2016) Being right on Q: shaping eukaryotic evolution. *Biochem J* 473:4103-27.
- 1661 Sugiura A, Mattie S, Prudent J, McBride HM (2017) Newly born peroxisomes are a hybrid of mitochondrial and
1662 ER-derived pre-peroxisomes. *Nature* 542:251-4.
- 1663 Simson P, Jepihhina N, Laasmaa M, Peterson P, Birkedal R, Vendelin M (2016) Restricted ADP movement in
1664 cardiomyocytes: Cytosolic diffusion obstacles are complemented with a small number of open mitochondrial
1665 voltage-dependent anion channels. *J Mol Cell Cardiol* 97:197-203.
- 1666 Stucki JW, Ineichen EA (1974) Energy dissipation by calcium recycling and the efficiency of calcium transport
1667 in rat-liver mitochondria. *Eur J Biochem* 48:365-75.
- 1668 Tonkonogi M, Harris B, Sahlin K (1997) Increased activity of citrate synthase in human skeletal muscle after a
1669 single bout of prolonged exercise. *Acta Physiol Scand* 161:435-6.

- 1670 Vamecq J, Schepers L, Parmentier G, Mannaerts GP (1987) Inhibition of peroxisomal fatty acyl-CoA oxidase by
1671 antimycin A. *Biochem J* 248:603-7.
- 1672 Waczulikova I, Habodaszova D, Cagalinec M, Ferko M, Ulicna O, Mateasik A, Sikurova L, Ziegelhöffer A
1673 (2007) Mitochondrial membrane fluidity, potential, and calcium transients in the myocardium from acute
1674 diabetic rats. *Can J Physiol Pharmacol* 85:372-81.
- 1675 Wagner BA, Venkataraman S, Buettner GR (2011) The rate of oxygen utilization by cells. *Free Radic Biol Med*
1676 51:700-712.
- 1677 Wang H, Hiatt WR, Barstow TJ, Brass EP (1999) Relationships between muscle mitochondrial DNA content,
1678 mitochondrial enzyme activity and oxidative capacity in man: alterations with disease. *Eur J Appl Physiol*
1679 *Occup Physiol* 80:22-7.
- 1680 Watt IN, Montgomery MG, Runswick MJ, Leslie AG, Walker JE (2010) Bioenergetic cost of making an
1681 adenosine triphosphate molecule in animal mitochondria. *Proc Natl Acad Sci U S A* 107:16823-7.
- 1682 Weibel ER, Hoppeler H (2005) Exercise-induced maximal metabolic rate scales with muscle aerobic capacity. *J*
1683 *Exp Biol* 208:1635-44.
- 1684 White DJ, Wolff JN, Pierson M, Gemmell NJ (2008) Revealing the hidden complexities of mtDNA inheritance.
1685 *Mol Ecol* 17:4925-42.
- 1686 Wikström M, Hummer G (2012) Stoichiometry of proton translocation by respiratory complex I and its
1687 mechanistic implications. *Proc Natl Acad Sci U S A* 109:4431-6.
- 1688 Willis WT, Jackman MR, Messer JI, Kuzmiak-Glancy S, Glancy B (2016) A simple hydraulic analog model of
1689 oxidative phosphorylation. *Med Sci Sports Exerc* 48:990-1000.
- 1690